Primary production in the Arctic Ocean, 1998–2006

Sudeshna Pabi,[1] Gert L. van Dijken,[1] and Kevin R. Arrigo[1]

Received 5 October 2007; revised 25 April 2008; accepted 19 May 2008; published 5 August 2008.

[1] Sea ice in the Arctic Ocean has undergone an unprecedented reduction in area and thickness in the last decade, exposing an ever increasing fraction of the sea surface to solar radiation and increasing the habitat suitable for phytoplankton growth. Here we use a primary production algorithm that utilizes remotely sensed chlorophyll *a*, sea surface temperature, and sea ice extent data to quantify interannual changes in phytoplankton production in the Arctic Ocean between 1998 and 2006. Our results show that since 1998, open water area in the Arctic has increased at the rate of 0.07×10^6 km^2 a^{-1} (where a is years), with the greatest increases in the Barents, Kara, and Siberian sectors, particularly over the continental shelf. Although pan-Arctic primary production averaged 419 ± 33 Tg C a^{-1} during 1998–2006, recent increases in open water area have lead to higher rates of annual production, which reached a 9-year peak in 2006. Annual production was roughly equally distributed between pelagic waters (less productive but greater area) and waters located over the continental shelf (more productive but smaller area). Interannual differences are most tightly linked to changes in sea ice extent, with changes in sea surface temperature (related to the Arctic Oscillation) and incident irradiance playing minor roles. Estimation of primary production in the Arctic will aid the assessment of air-sea CO_2 fluxes and improve our understanding of the ecological and biogeochemical changes that could take place if ice cover continues to decrease.

Citation: Pabi, S., G. L. van Dijken, and K. R. Arrigo (2008), Primary production in the Arctic Ocean, 1998–2006, *J. Geophys. Res.*, *113*, C08005, doi:10.1029/2007JC004578.

1. Introduction

[2] The Arctic Ocean is currently in the forefront of climate change caused by both natural and anthropogenic factors. Since 1950, the mean annual air temperature has increased by 2–3°C and by 4°C in winter [*Chapman and Walsh*, 1993], resulting in markedly longer summers [*Smith*, 1998]. Temperature is projected to increase by an additional 4–5°C by the end of the 21st century [*Arctic Climate Impact Assessment* (*ACIA*), 2005]. In conjunction with these higher temperatures, sea ice cover in the Arctic Ocean has been contracting over the past three decades, with dramatic reductions in recent years [*Levi*, 2000; *Parkinson*, 2000]. Changes in sea ice cover also include an increase in the length of the ice melt season [*Smith*, 1998; *Rigor et al.*, 2002; *Serreze et al.*, 2007; *Comiso et al.*, 2008] and a decrease in ice thickness over the central Arctic Ocean [*Rothrock et al.*, 1999]. The result is greater open water area and enhanced shelf break upwelling, the latter of which is expected to increase the input of nutrients from offshore waters to shallower shelves [*ACIA*, 2005]. While a reduction in sea ice should favor the growth of phytoplankton and increase the net air-to-sea flux of CO_2 [*Anderson and Kaltin*, 2001; *Bates et al.*, 2006], it also will reduce the amount of production contributed by algae growing within the sea ice [*Subba Rao and Platt*, 1984; *Legendre et al.*, 1992; *Gosselin et al.*, 1997], although sea ice communities generally account for a relatively small fraction of total primary production in Arctic waters.

[3] One step toward a better understanding of the effects of these environmental changes on the marine ecosystem and carbon biogeochemistry in the Arctic is to quantify current rates of basin-scale phytoplankton primary production. While a number of primary production estimates are already available for the Arctic [e.g., *Platt et al.*, 1982; *Wassmann and Slagstad*, 1993; *Vedernikov et al.*, 1994; *Gosselin et al.*, 1997; *Boetius and Damm*, 1998; *Tremblay et al.*, 2002], these cover relatively small temporal and spatial scales. This is primarily due to the difficulty of sampling such a harsh and often inaccessible environment. The data that are available suggest that rates of primary production in this region are governed by its unique physical environment. For example, the shallow bathymetry of much of the Arctic Ocean greatly influences the light and nutrient inventories that are required for primary production. Discharge from rivers both enhances primary production by supplying additional nutrients and inhibits it by limiting light transmission through the water column due to high sediment loads [*Kirk*, 1983]. Sea ice also impacts light transmission to the water column and plays a crucial role in determining the mixed layer depth (via increased stratification during ice melt and convective mixing during sea ice formation) that, along with the critical depth, dictates the

[1]Department of Environmental Earth System Science, Stanford University, Stanford, California, USA.

0148-0227/08/2007JC004578$09.00

onset and demise of the spring and summer phytoplankton blooms.

[4] Unlike other oceans, the Arctic Ocean is almost completely landlocked, except for the very shallow Bering Strait (~50 m), that connects it to the Pacific Ocean, and the Fram Strait and Canadian Archipelago that allow exchange with the Atlantic Ocean. Associated with the extensive land margin is a broad continental shelf, 5×10^6 km^2 in area, and comprising about 53% of the total Arctic Ocean. This is much higher than the 9.1−17.7% characteristic of continental shelves in other oceans of the world [*Menard and Smith*, 1966; *Jakobsson et al.*, 2003]. Ice-free continental shelves, such as those found in parts of the Chukchi Sea, often experience intense seasonal blooms of phytoplankton owing to their favorable nutrient and light conditions [*Hill and Cota*, 2005].

[5] Another unique feature of the Arctic Ocean is the large amount of riverine discharge it receives (~4000 km^3 a^{-1} (where a is years)) [*Shiklomanov*, 2000; *Carmack and Macdonald*, 2002], arising from both large rivers, like the Ob, Lena, Yenisey, and Mackenzie, and numerous smaller ones in both the Amerasian and Eurasian sectors. This large freshwater input affects both the salinity and nutrient concentration of the Arctic Ocean. Furthermore, it is predicted that precipitation in a warming climate will increase significantly [*Intergovernmental Panel on Climate Change*, 2007], thereby enhancing the already enormous fluxes of riverine sediment discharge (670 Mt a^{-1}) and organic carbon (12.6 Mt a^{-1}) from the land to the Arctic Ocean [*Macdonald et al.*, 1998], both of which will impact nutrient and light availability and hence, phytoplankton growth.

[6] The circulation of the Arctic Ocean is composed of both low salinity (<33) and nutrient-rich Pacific Ocean water and relatively nutrient-poor and more saline (~34.8) Atlantic Ocean water [*Maslowski et al.*, 2004]. The denser Atlantic water is distributed via counterclockwise currents along the continental slope at the basin margins. The relatively less saline and warmer Pacific water enters the Arctic Basin through the Bering Strait between Cape Dezhnev and west Alaska, and exits through the Canadian Archipelago, the Fram Strait, and the Nares Strait. Historically, the front separating the Atlantic and Pacific water has been located over the Lomonosov Ridge, but recently this front appears to have moved closer to the Alpha-Mendeleev Ridge. This shift in the location of the front has lead to the displacement of a large quantity of Pacific water that has been replaced by nutrient-poor water from the Atlantic [*Macdonald*, 1996], potentially reducing the amount of nutrients available for phytoplankton growth. The nutrient-rich water from the Pacific Ocean is generally restricted to the Chukchi Sea and the Amerasian Basin [*Carmack et al.*, 1997].

[7] Surface concentrations of nitrate, phosphate and silicic acid in Arctic waters approach detection limits after the spring bloom [*Sakshaug*, 2003], suggesting that annual primary production is generally controlled by nutrient availability. The nitrate to phosphate ratio in these waters ranges from 11 to 16 (mol:mol) [*Sakshaug*, 2003], suggesting that much of the Arctic Ocean is nitrogen limited (assuming that phytoplankton require nitrogen and phosphorus at the Redfield ratio of 16:1). Phosphorus limitation of phytoplankton is more likely in waters with a salinity of <25 [*Sakshaug et al.*, 1983] due to low phosphate content of river waters that are otherwise rich in nitrate. The silicic acid to nitrate molar ratio is spatially variable, ranging from a high of 1.9−2.4 in the Chukchi Sea and Eastern Canadian Arctic to a low of 0.31 in the Eurasian basin [*Codispoti*, 1979; *Harrison and Cota*, 1991; *Sakshaug*, 2003].

[8] Finally, sea ice dynamics are integral to the regulation of primary production in much of the Arctic Ocean. In winter, brine rejection due to ice formation destabilizes the mixed layer, leading to deep vertical mixing and replenishment of surface nutrient inventories. In spring, melting of ice results in strong surface ocean stratification, exposing the nutrient-rich waters to a light regime suitable for phytoplankton growth. The resulting spring ice edge bloom forms a significant component of the annual primary production [*Niebauer et al.*, 1990; *Falk-Petersen et al.*, 2000]. In the study presented here, we assessed seasonal and interannual changes in the physical characteristics of the Arctic Ocean, including changes in irradiance, sea surface temperature, and sea ice distributions. In addition, we quantified the changes in phytoplankton chlorophyll *a* (Chl *a*) and primary production that accompanied interannual differences in the physical environment of the Arctic Ocean within a number of different ecological provinces (e.g., pelagic and continental shelf). This was accomplished using a primary production algorithm parameterized for the Arctic Ocean with input data from a number of satellite remote sensing platforms. This approach has the advantage of providing estimates of Arctic primary production at relatively high temporal resolution over large geographic areas.

2. Methods

2.1. Primary Production Algorithm

[9] Daily primary productivity (PP, mg C m^{-2} d^{-1}) at each satellite pixel location was computed by integrating over depth z (0−100 m at 1 m intervals) and time t (hourly for 24 h) as described in detail by *Arrigo et al.* [1998] and modified by *Arrigo et al.* [2008]. In its simplest form, the governing equation can be represented as

$$\mathrm{PP} = \int_{z=0}^{100} \int_{t=0}^{24} \mathrm{Chl}(z) \frac{C}{\mathrm{Chl}} G(z,t) dt dz, \qquad (1)$$

where $G(z, t)$ is the net biomass-specific phytoplankton growth rate (hr^{-1}) and C/Chl is the phytoplankton carbon to Chl *a* ratio (90 g:g, see below). Surface Chl *a* concentrations determined from 8-day Sea-viewing Wide Field-of-view Sensor (SeaWiFS) Level 3 (L3) images are considered to be representative of concentrations throughout the mixed layer. Below the mixed layer, Chl *a* is assumed to decrease exponentially with depth as described by *Arrigo et al.* [2008]. In the Arctic, the spring-summer mixed layer depth (MLD) is reported to vary between 15 and 20 m [*McLaughlin et al.*, 2005]. In the present study, the MLD is assumed to be 20 m, similar to the value used by *Walsh et al.* [2005]. Sensitivity studies revealed that the algorithm is not sensitive to MLD; for example, increasing the MLD to 50 m increased the calculated depth-integrated primary production by only 10%. $G(z, t)$ is calculated each hour (t)

and at each depth (z) as a function of the temperature-dependent upper limit to net growth and a light limitation term, L (dimensionless)

$$G(z,t) = G_o \exp[rT(t)]L(z,t), \quad (2)$$

where G_o is the maximum microalgal net growth rate at 0°C (0.59 d^{-1}) and r is a rate constant (0.0633°C^{-1}) that determines the sensitivity of G to temperature, T (°C) [*Eppley*, 1972]. The light limitation term, $L(z, t)$, is calculated for each depth and each hour as

$$L(z,t) = 1 - \exp\left(-\frac{\mathrm{PUR}(z,t)}{E'_k(z,t)}\right), \quad (3)$$

where PUR(z, t) is photosynthetically usable radiation [*Morel*, 1978, 1987, 1991] and $E'_k(z, t)$ is the spectral photoacclimation parameter [*Arrigo and Sullivan*, 1994]. PUR is similar to photosynthetically active radiation (PAR, the total radiation between 400 and 700 nm), except that PUR is weighted by the phytoplankton specific absorption spectra, as described by *Morel* [1978], and represents the subset of PAR that is readily absorbed by phytoplankton. $E'_k(z, t)$ varies with light history, simulating phytoplankton photoacclimation to a changing light regime. Downwelling spectral irradiance at the ocean surface was determined using the radiative transfer model of *Gregg and Carder* [1990], corrected for fractional cloud cover (from NCEP Reanalysis data) and specular reflectance [*Arrigo et al.*, 2008]. Downwelling spectral irradiance was propagated through the water column according to Beer's law as described by *Arrigo et al.* [1998] using the inherent optical properties typical of this ocean [*Wang and Cota*, 2003].

2.2. Algorithm Input Data

2.2.1. Chlorophyll *a*

[10] Surface Chl *a* concentrations were determined from Level 3 (9 km resolution) SeaWiFS ocean color data (operational August 1997–present, distributed by http://oceancolor.gsfc.nasa.gov/) using the OC4v4 algorithm [*O'Reilly et al.*, 1998]. The OC4v4 Chl *a* algorithm is suitable for Case I waters where the optical properties are dominated primarily by Chl *a*. However, we recognize that a large sediment load as well as CDOM from river discharge has the potential to alter these optical properties and impact Chl *a* retrievals. Hence, to account for the influence of riverine sediments in coastal waters, primary production was quantified both by including and excluding questionable SeaWiFS pixels that were in proximity to the river discharge plumes (these pixels were flagged as being turbid in the SeaWiFS data). Because exclusion of pixels associated with river discharge reduced the pan-Arctic primary production by less than 10%, all results reported here have had river-influenced pixels removed.

[11] In addition, SeaWiFS data for the Arctic Ocean are only available from March through September, after which the SeaWiFS sensor begins focusing its data collection and storage on more southerly waters. Because irradiance is minimal outside this data collection period, the lack of SeaWiFS data at other times of year is likely to result in only a slight underestimate of annual primary production (<10%).

2.2.2. Sea Surface Temperature

[12] Sea surface temperature (SST) is based on the Reynolds Optimally Interpolated SST (OISST) Version 2 product [*Reynolds et al.*, 2002] obtained from NOAA (http://www.emc.ncep.noaa.gov/research/cmb/sst_analysis/).

2.2.3. Open Water Area

[13] Open water area was estimated from Special Sensor Microwave Imager (SSM/I) 37 and 85 GHz bands using the Polynya Signature Simulation Method (PSSM) algorithm [*Markus and Burns*, 1995] which allows determination of sea ice presence/absence at 6.25 km resolution. A given pixel is defined as being ice covered wherever the sea ice concentration is greater than approximately 10%.

[14] All satellite remote sensing data were processed using Interactive Data Language (IDL). The primary productivity algorithm was encoded using Fortran 77. All computations were done at the High Productivity Technical Computing facility of Stanford University Center of Computational Earth and Environmental Science, which is composed of a Sun Sparc cluster running Solaris 10.

2.3. Defining Regions of Interest

[15] The Arctic Ocean is defined as all waters north of the Arctic Circle (66°33′39″). For the purpose of characterizing spatial differences, we divided the Arctic Ocean into eight geographic sectors and four open water ecological regimes. The geographic sectors were demarcated by longitude (Figure 1a) and include the Chukchi (180–160°W), Beaufort (160–100°W), Baffin (100–45°W), Greenland (45°W–15°E), Barents (15–55°E), Kara (55–105°E), Laptev (105–150°E), and Siberian (150–180°E) sectors.

[16] The four ecological provinces include the pelagic, the shelf, the deep water marginal ice zone (DMIZ) and the marginal ice zone (MIZ) over the continental shelf (SMIZ). All provinces vary in size over time because of continual changes in sea ice extent (Figure 1b). The ecological provinces were demarcated using a combination of sea ice distributions and bathymetric information. The pelagic and shelf provinces are defined as those waters with depths of >220 m and ≤220 m, respectively (in accordance with the definition of the Arctic continental shelf by *Walsh et al.* [2005]), and that have remained ice free for >14 consecutive days. A pixel is considered part of the MIZ if it has been ice free for ≤14 days [*Arrigo et al.*, 2008]. If an MIZ pixel is located on the shelf, then it is defined as belonging in the SMIZ, otherwise it is defined as being part of the DMIZ. The SMIZ and DMIZ together constitute the total Arctic Ocean MIZ.

2.4. Algorithm Validation

[17] In the present study, we chose to use the surface Chl *a* concentrations produced from SeaWiFS data by the standard OC4v4 algorithm [*O'Reilly et al.*, 1998] rather than the regional Arctic algorithm of *Wang and Cota* [2003]. This decision was based on a recent assessment by *Matsuoka et al.* [2005], who used measurements of in-water apparent optical properties and Chl *a* to show that the standard OC4v4 Chl *a* algorithm used with SeaWiFS data performs as well or better in Arctic waters than the algorithm of *Wang and Cota* [2003]. The two algorithms exhibited root mean square (RMS) errors between in situ and satellite-derived Chl *a* of 25% and 30%, respectively.

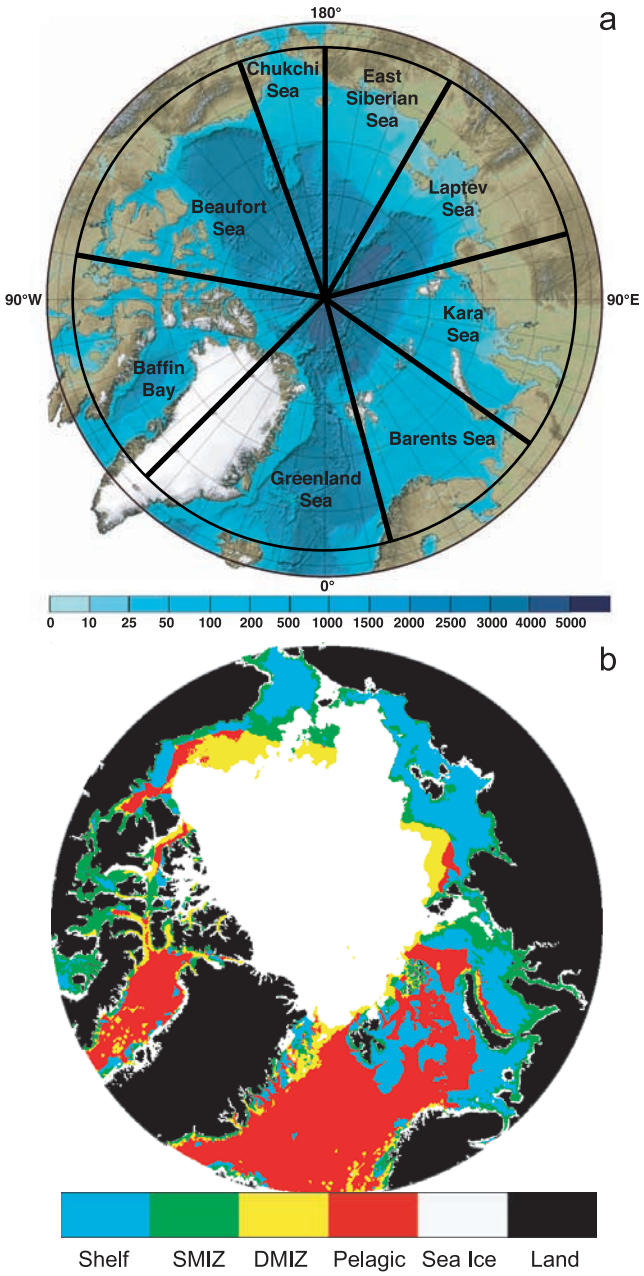

Figure 1. Map of the study area showing (a) bathymetry (in m), the location of the Arctic Circle (shown in black), and the distribution of the eight geographic sectors (map adapted from the International Bathymetric Chart of the Arctic Ocean [*Jakobsson et al.*, 2008]) and (b) an example of the locations of the four ecological provinces (September 1998).

[18] The best way to validate our primary production algorithm would be to compare algorithm-derived production with in situ estimates of primary production made at the same time and location. However, because of the small number of cloud-free images that correspond to available in situ measurements in the Arctic, this approach is not feasible. Thus, to validate our primary production algorithm we assumed that retrievals of surface Chl *a* by SeaWiFS were reliable (in waters not influenced by river runoff) and then compared regressions of daily primary production against surface Chl *a* produced by our algorithm to similar regressions generated from in situ Arctic data.

[19] In situ measurements of primary production and concurrent surface Chl *a* concentrations used in this analysis were obtained from Phase I and II of the Shelf Basin Interaction (SBI) program (http://www.eol.ucar.edu/projects/sbi/) conducted in the Chukchi and Beaufort sectors of our study area during 2002–2004. The relationship between surface Chl *a* and daily primary production predicted by our algorithm for the SBI study region agrees well with the in situ data, particularly in spring (Figure 2a). In summer, there are clear cases where the algorithm underestimates daily production at low surface Chl *a* concentrations (Figure 2b). These were stations with a particularly strong subsurface Chl *a* maximum [*Hill and Cota*, 2005], which was not detected by the SeaWiFS sensor. Unfortunately, the prevalence of subsurface Chl *a* maxima in the Arctic Ocean is not well known so the significance of the problem cannot be adequately determined at this time.

[20] The relationship between surface Chl *a* and computed primary production is sensitive to the value used for the C:Chl *a* ratio. A value of 90 produced the best agreement between algorithm-derived and in situ primary production. This is encouraging because 90 is similar to the C:Chl *a* ratio determined to be optimal for computing primary production in the Southern Ocean (88.5) using the same algorithm as that used here [*Arrigo et al.*, 2008]. It is also well within the range of 25–100 reported for in situ C:Chl *a* measurements from the Arctic [*Platt et al.*, 1982; *Buck et al.*, 1998; *Sakshaug*, 2003]. Although the paucity of Arctic data makes it difficult to validate our algorithm across the full range of surface Chl *a* values that have been measured, our algorithm has been validated over a much larger range of Chl *a* concentrations and rates of daily primary production in the Southern Ocean [*Arrigo et al.*, 2008], further supporting its use in northern polar waters.

3. Results

3.1. Interannual Ice Dynamics

3.1.1. Pan-Arctic

[21] During the 9-year period of interest (POI) of this study (1998–2006), the annual mean open water (ice-free) area in the Arctic Ocean exhibited a dramatic and statistically significant upward trend ($R^2 = 0.78$, $p = 0.002$), increasing at the rate of $\sim 0.07 \times 10^6$ km^2 a^{-1} (Figure 3a). This trend is consistent with earlier studies reporting a substantial loss of sea ice in recent decades, with Arctic ice cover decreasing by $\sim 0.80 \times 10^6$ km^2 (7.4%) between 1978 and 2002 [*Johannessen et al.*, 1999; *Cavalieri et al.*, 2003]. Open water area during the POI was at its 9-year low in 1998, averaging $\sim 3.8 \times 10^6$ km^2 over the year; the maximum annual mean open water area was attained in 2006, averaging 4.6×10^6 km^2. Although annual mean open water area in the Arctic increased by 19% between 1998 and 2006, this increase was not uniform throughout the year. For example, during August–September (the peak open water season, Figure 4a), open water area averaged $6.9 \pm 0.03 \times 10^6$ km^2 during the POI, and increased by 11% between 1998 and 2006 (Figure 3c). However, during May–June

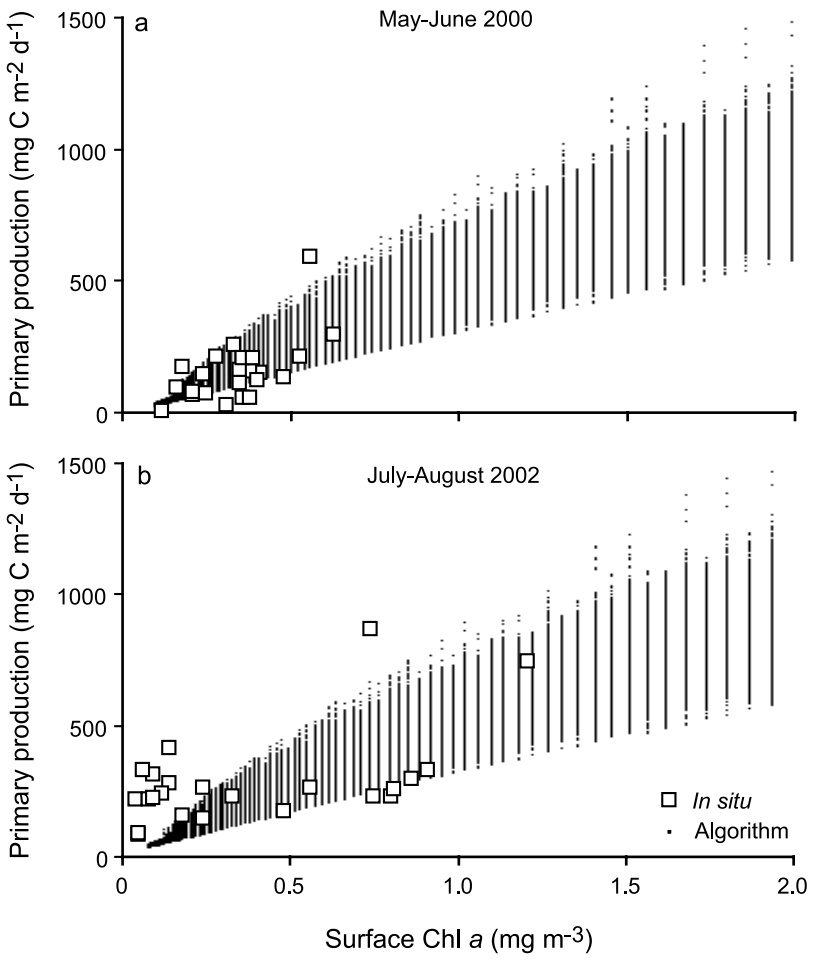

Figure 2. Plots of surface Chl *a* versus daily primary production estimated from our primary production algorithm and measured in situ at discrete stations from the Chukchi and Beaufort seas obtained during the Shelf Basin Interaction program during (a) May–June 2002 and (b) July–August 2002. Algorithm output used in this analysis was restricted to those times and locations for which in situ data were available.

(the peak of the spring phytoplankton bloom), open water area averaged only $3.3 \pm 0.02 \times 10^6$, but the change over time was more pronounced than in summer, increasing by 26% between 1998 and 2006 (Figure 3b). This pattern reflects the fact that in recent years, Arctic sea ice has been retreating progressively earlier in the year.

[22] Recent increases in annual mean open water area in the Arctic are the result of changes in both the timing of sea ice advance and retreat (earlier retreat and later advance will result in higher annual mean open water area) and the maximum amount of open water area attained during the year. For example, the relatively large annual mean open water area observed in 2002 and 2005 were due mainly to the extensive open water area in summer. On the other hand, open water area in the summer was actually lower in 2006 (the lightest sea ice year) than it was in 2005 (Figure 3c). However, the retreat of sea ice began relatively early in 2006 and the advance began later (Figure 4a), more than compensating for the low summertime open water area. The early retreat of sea ice in recent years appears to be coupled with the higher early season SST, particularly in 2005 and 2006 (Figure 4b). The annual mean SST in the Arctic Ocean increased from −0.07°C in 1998 to +0.26°C in 2006. Unfortunately, it is not clear from these data whether higher SST led to the increase in open water area or vice versa. However, the peak in SST (Figure 4b) correlates well with the timing of peak open water area (Figure 4a), with the latter lagging the annual SST peak by approximately 20 days.

3.1.2. Geographic Sectors

[23] Among all geographic sectors, the Greenland and Barents had the largest annual mean open water area, averaging $\sim 1.6 \pm 0.36 \times 10^6$ km^2 and $\sim 1.1 \pm 0.11 \times 10^6$ km^2, respectively (Figure 5) during the POI. Whereas open water area in most sectors was reduced to near zero in winter, the Barents and Greenland sectors had significant amounts of permanently open water (Figure 12c), which appears to have increased in the Barents sector in recent years. The lowest annual mean open water area in the Arctic was observed in the Siberian and Laptev sectors, averaging only $0.18 \pm 0.06 \times 10^6$ km^2 and $0.22 \pm 0.06 \times 10^6$ km^2, respectively. Interannual differences in annual mean open water area were most dramatic in the Eurasian sectors, with the annual mean open water area in the Siberian, Laptev and

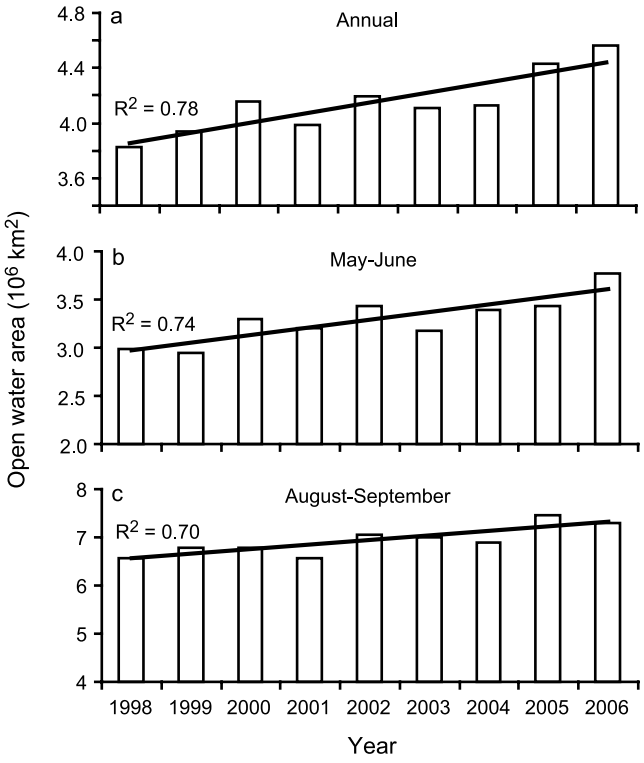

Figure 3. Open water area in the Arctic Ocean averaged over (a) the entire year, (b) the months of May–June (time of the a spring bloom), and (c) the months of August–September (time of maximum open water). Also shown is the long-term trend in mean open water area.

Kara sectors being 276%, 134%, and 114% higher, respectively, in their lightest sea ice year than in their heaviest.

[24] Over the POI, the rate of change in open water area varied substantially by geographic sector (Figure 5). The Barents, Kara and Siberian sectors experienced greater absolute increases in open water area than any other sector, with the annual mean open water area increasing at a rate of 25,047 km^2 a^{-1} (about 2% of the 1998 extent), 20,046 km^2 a^{-1} (about 10% of the 1998 extent), and 14,416 km^2 a^{-1} (about 30% of the 1998 extent), respectively, over the POI, although this increase was only statistically significant in the Siberian sector. In other sectors, open water area increased at a rate of only ~5,000 km^2 a^{-1} (except for the Beaufort, where open water area decreased over time). The relative increase in open water area was largest in the Siberian sector, increasing 276% between 1998 (0.05×10^6 km^2) and 2005 (0.19×10^6 km^2). In terms of absolute area, the Barents sector experienced the largest rise in open water area, increasing by 0.36×10^6 km^2 between 1998 and 2006. Despite having the largest open water area of all the geographic sectors, changes in open water area in the Greenland sector were far less dramatic, with the minimum and maximum open water years (1998 and 2004, respectively) differing by only 7%. This small change is due to a large area of permanently open water within the pelagic province that has persisted throughout the POI. Interestingly, open water area in the Beaufort sector actually dropped during the POI, decreasing by 178% over the 9-year study period, from a maximum area of 0.38×10^6 km^2 in 1998 to a minimum of 0.12×10^6 km^2 in 2001. However, this trend was dominated by the large drop in ice cover between 1998 and 1999 (Figure 5c). Since then, interannual changes in open water area in the Beaufort have been small.

3.1.3. Ecological Provinces

3.1.3.1. Annual Mean Open Water Area

[25] The largest ecological province in the Arctic Ocean is the pelagic, encompassing an annual mean area of $2.16 \pm 0.07 \times 10^6$ km^2 during the POI (Figure 5a). In the Greenland and the Barents sectors, the pelagic province comprises 82% (1.34×10^6 km^2) and 47% (0.53×10^6 km^2), respectively, of the total open water area in these sectors (Figures 5e and 5f). The Baffin and Beaufort sectors also have significant pelagic provinces, covering 45% (0.18×10^6 km^2) and 25% (0.05×10^6 km^2), respectively, of their total area during the POI (Figures 5c and 5d).

[26] The shelf province is the second largest ecological province in the Arctic Ocean with an annual mean open water area of $0.90 \pm 0.1 \times 10^6$ km^2 (Figure 5a). The two geographic sectors with the largest shelf province (in

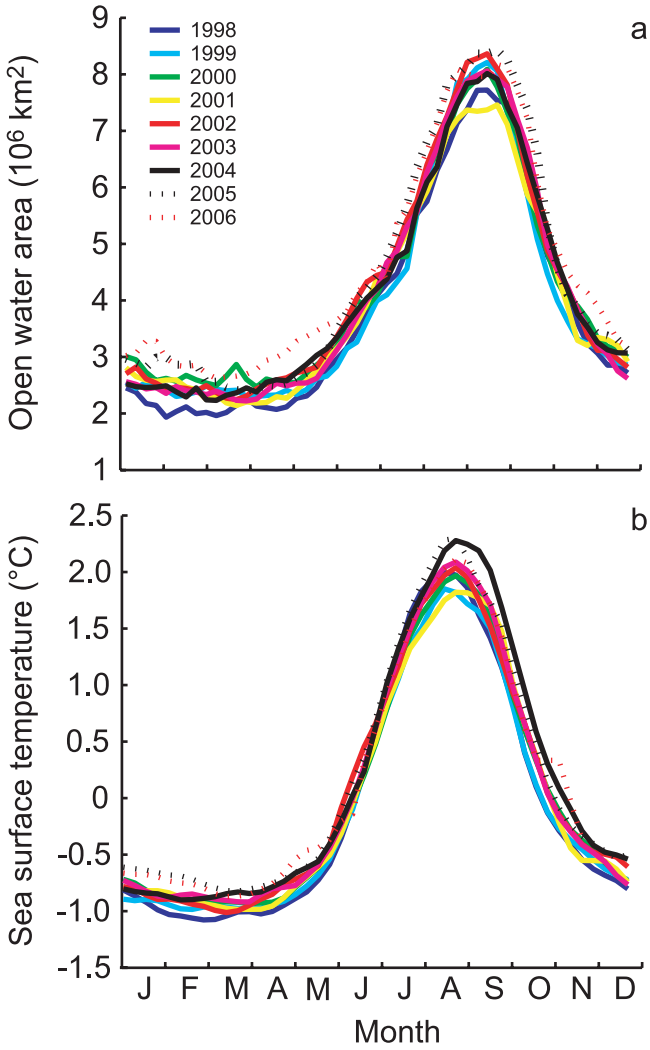

Figure 4. Weekly changes in (a) open water area and (b) sea surface temperature during 1998–2006.

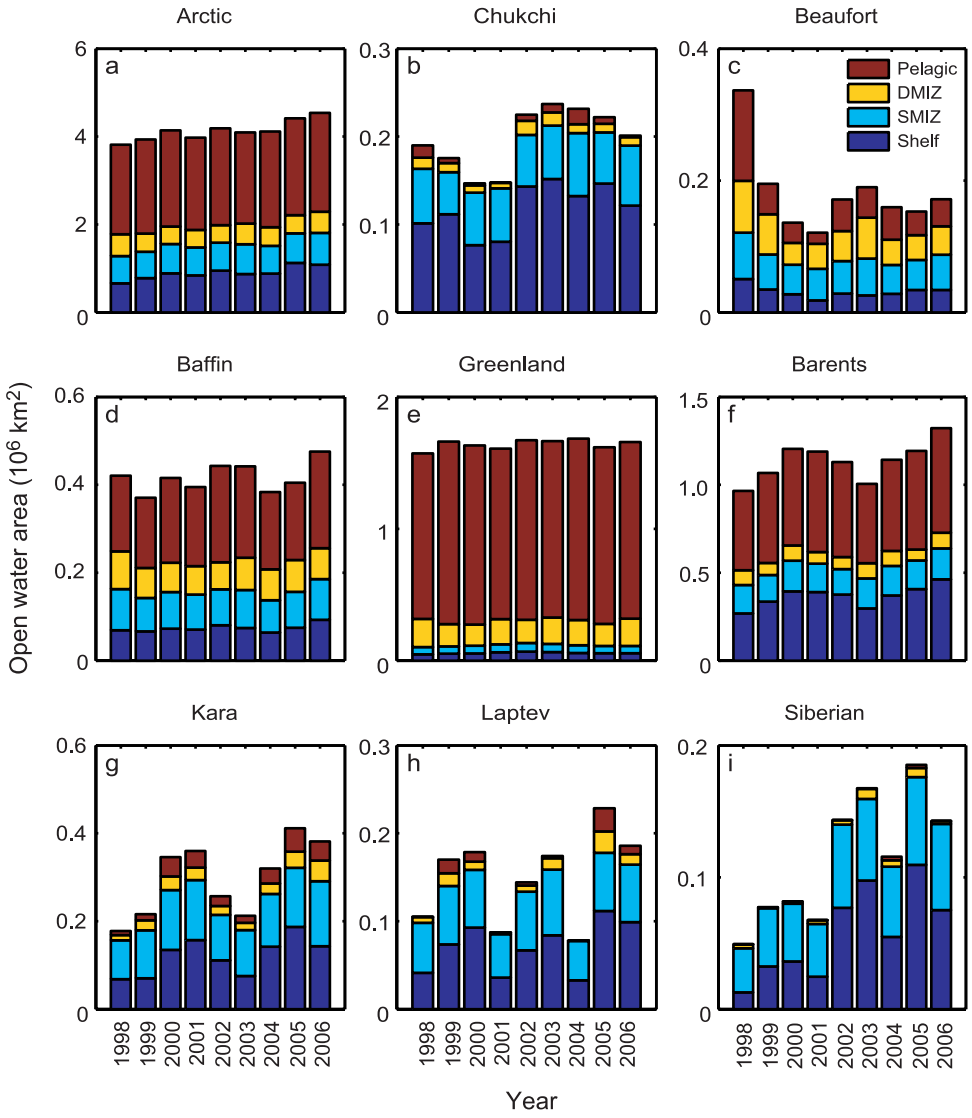

Figure 5. Annual mean open water area in the Arctic Ocean for each ecological province and geographical sector during 1998–2006.

absolute area) were the Barents and Chukchi (Figures 5b and 5f), where open water area averaged 0.37 × 10^6 km^2 (32% of annual mean open water area in that sector) and 0.12 × 10^6 km^2 (59% of annual mean open water area in that sector), respectively, during the POI. Other geographic sectors with substantial shelf provinces were the Siberian, Laptev, and Kara sectors, where the shelf comprised 47% (0.05 × 10^6 km^2), 46% (0.07 × 10^6 km^2), and 39% (0.12 × 10^6 km^2), respectively, of total open water area in their respective sectors during the POI.

[27] The area of the SMIZ province was slightly smaller than the shelf province, with an annual mean open water area of 0.70 ± 0.04 × 10^6 km^2 (Figure 5a). Geographic sectors with a relatively large SMIZ include the Siberian, Laptev, Kara and Chukchi sectors, where the SMIZ was nearly as large as the shelf province, averaging 49% (0.05 × 10^6 km^2), 44 % (0.06 × 10^6 km^2), 41% (0.12 × 10^6 km^2) and 31% (0.06 × 10^6 km^2), respectively, of total open water area during the POI. The largest SMIZ in terms of absolute area was in the Barents sector, averaging 0.16 × 10^6 km^2, although it comprised only 14% of the total open water area in that sector.

[28] The DMIZ is the smallest of the four ecological provinces, averaging just 0.43 ± 0.04 × 10^6 km^2 over the POI (Figure 5a). The DMIZ was largest in the Greenland sector, where it averaged 0.19 × 10^6 km^2, nearly 50% of the total DMIZ area of the Arctic. This province was also relatively large in the Beaufort sector (0.08 × 10^6 km^2), where it comprised 27% of the open water area, and in the Barents (0.05 × 10^6 km^2) and Baffin sectors (0.07 × 10^6 km^2) where it comprised 17% of open water area.

3.1.3.2. Changes Over Time

[29] Open water area in the pelagic province of the Arctic Ocean typically increases from a winter low of 1.2–1.7 × 10^6 km^2 (range reflects values for different years) to a peak of 3.2–3.6 × 10^6 km^2 some time between late August and late October (Figure 6). Winter ice cover is much heavier in the other ecological provinces, such as the shelf, where open water area increased by an order of magnitude from a January minimum of only 0.12–0.30 × 10^6 km^2 to a

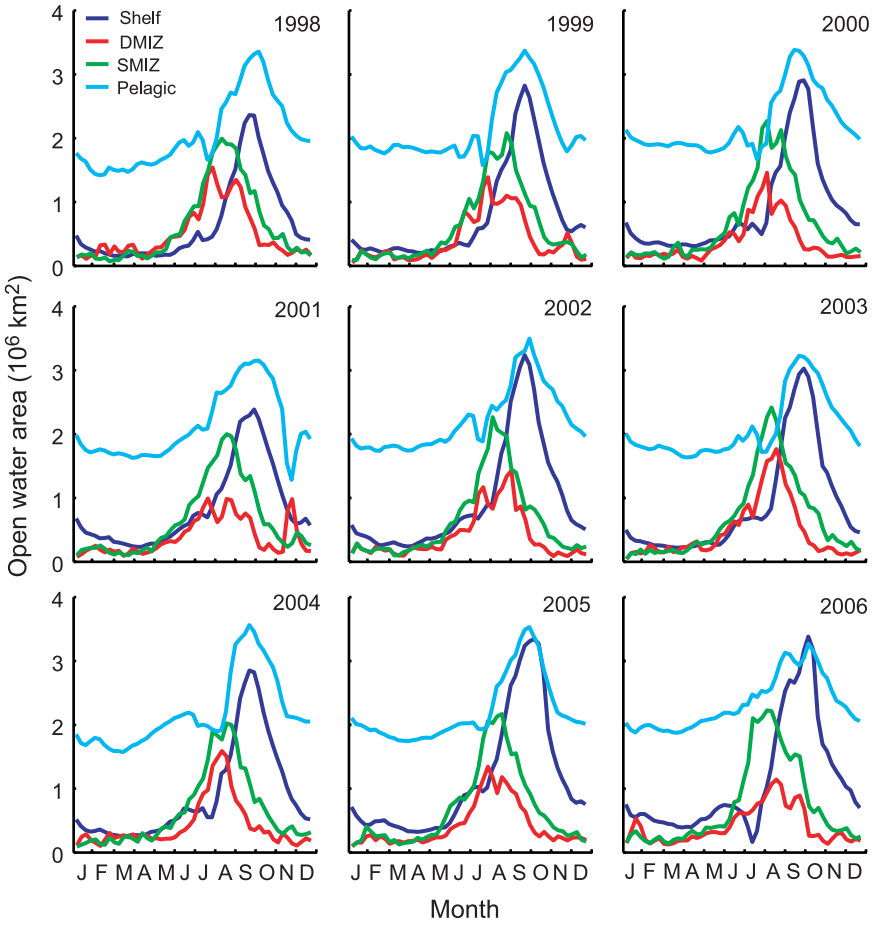

Figure 6. Weekly changes in open water area in the four ecological provinces of the Arctic Ocean during 1998–2006.

maximum of 2.4–3.4 $\times$ 10^6 km^2 in early September to late October. The open water area in the SMIZ and DMIZ increased even more dramatically, rising seasonally by 2 orders of magnitude, from a low of 0.02–0.09 $\times$ 10^6 km^2 and 0.01–0.07 $\times$ 10^6 km^2, respectively, in January to a peak of 2.1–2.6 km^2 and 1.2–2.5 $\times$ 10^6 km^2, respectively, during the peak open water period (mid-July to early September). The length of the open water period in the shelf, SMIZ, and DMIZ provinces were in general shorter than that of the pelagic province.

[30] The annual mean open water area in the pelagic province of the Arctic increased annually at a rate of 0.17 $\times$ 10^6 km^2 a^{-1} (R^2 = 0.42) between 1998 and 2006, although this increase is not statistically significant (p = 0.06, Table 1). Although smaller in area, the secular increase in annual mean open water area during the POI in both the shelf and the SMIZ provinces was significant, increasing annually at a rate of 0.05 $\times$ 10^6 km^2 a^{-1} (R^2 = 0.77, p = 0.002) and 0.01 $\times$ 10^6 km^2 a^{-1} (R^2 = 0.55, p = 0.02), respectively (Table 1). Secular increases in open water area were most dramatic in the shelf and the SMIZ zones of the Siberian sector (Table 1), increasing at a rate of 0.010 $\times$ 10^6 km^2 a^{-1} (R^2 = 0.64, p = 0.01) and 0.004 $\times$ 10^6 km^2 a^{-1} (R^2 = 0.75, p = 0.02), respectively, during the POI (Table 1). These changes in the Siberian sector represent a ninefold increase in open water area (from a minimum of 0.012 $\times$ 10^6 km^2 in 1998 to maximum of 0.110 $\times$ 10^6 km^2 in 2005) in the shelf and a twofold increase (from a minimum of 0.033 $\times$ 10^6 km^2 in 1998 to maximum of 0.067 $\times$ 10^6 km^2 in 2005) in the SMIZ province between 1998 and 2006 (Figure 5i). Apart from these regions, there was no significant secular increase in open water area within the ecological provinces of any geographic sector of the Arctic during the POI (Table 1).

3.2. Primary Production

3.2.1. Pan-Arctic Primary Production

[31] Phytoplankton dynamics in the Arctic Ocean are characterized by an initial spring bloom in April–May, and in some years, a subsequent summer bloom during July–August (Figure 7a). Between these two blooms, mean surface Chl *a* concentrations in the Arctic remain relatively high, generally exceeding 1.5 mg m^{-3}. Surprisingly, the summer bloom was the more prominent of the two blooms during the first half of the POI (1998–2001), with the mean Chl *a* concentration during the summer bloom being comparable to or even exceeding that measured during spring. Between 2002 and 2004, this pattern was reversed, with Chl *a* concentrations in spring exceeding those in both summer and autumn. However, in the 2 most recent years, the intensity of the summer bloom had again increased, with

Table 1. Linear Regression of Open Water Area Against Year by Geographic Sector and Ecological Province[a]

	Chukchi	Beaufort	Baffin	Greenland	Barents	Kara	Laptev	Siberian	Arctic
				Shelf					
Slope	6131	−967	1762	898	14,190	9711	4552	**9841**	**46,110**
R^2	0.360	0.089	0.320	0.135	0.436	0.394	0.186	**0.635**	**0.768**
p Value	0.087	0.435	0.113	0.330	0.053	0.070	0.246	**0.010**	**0.002**
				SMIZ					
Slope	1328	−1425	19	102	1398	4202	288	**3937**	**9848**
R^2	0.298	0.225	0.000	0.005	0.145	0.336	0.007	**0.751**	**0.546**
p Value	0.128	0.197	0.984	0.850	0.312	0.102	0.833	**0.002**	**0.023**
				DMIZ					
Slope	−24	−2966	−563	523	332	2578	743	441	1063
R^2	0.000	0.284	0.049	0.006	0.007	0.431	0.081	0.262	0.005
p Value	0.956	0.140	0.568	0.848	0.832	0.055	0.459	0.159	0.850
				Pelagic					
Slope	−35	−5816	3872	4810	9138	3555	809	198	16,529
R^2	0.000	0.216	0.237	0.101	0.247	0.391	0.061	0.250	0.415
p Value	0.965	0.207	0.184	0.405	0.174	0.072	0.520	0.170	0.061
				Total					
Slope	7399	−11,174	5090	6333	25,047	20,046	6392	**14,416**	**73,550**
R^2	0.339	0.238	0.180	0.225	0.390	0.425	0.120	**0.680**	**0.780**
p Value	0.100	0.183	0.256	0.197	0.072	0.057	0.361	**0.006**	**0.002**

[a]Slopes are in units of $km^2\ a^{-1}$. Bolding denotes statistical significance at the 95% confidence level.

Chl *a* concentrations eclipsing those of the spring bloom in both 2005 (by a large margin) and 2006 (only slightly).

[32] The daily rate of area-normalized production over the entire Arctic basin during the POI averaged 420 ± 26 mg C $m^{-2}\ d^{-1}$ during the phytoplankton growing season from March through September. Rates were highest in 2006 and 2001, averaging 474 and 447 mg C $m^{-2}\ d^{-1}$, respectively (Figure 7a). The mean daily rate of area-normalized production was lowest in 1999 at 393 mg C $m^{-2}\ d^{-1}$. The daily rate of area-normalized production peaked during the May–June period (Figure 7c), correlating well with surface Chl *a* (Figure 7a) during the spring bloom when the amount of PAR incident on the sea surface is relatively high (Figure 7b). Despite occasionally high Chl *a* concentrations (Figure 7a), daily area-normalized rates of production (Figure 7c) were consistently lower during the summer months because of the dwindling irradiance characteristic of this time of year (Figure 7b).

[33] Although daily production in August–September (360 ± 33 mg C $m^{-2}\ d^{-1}$) was lower than in May–June (659 ± 39 mg C $m^{-2}\ d^{-1}$), the August–September values have a disproportionate impact on annual primary production (Figure 7d) because they coincide with the annual peak in open water area (Figure 4a). For instance, 2001 exhibited the highest August–September rates of area-normalized production of any year except 2006 (Figure 7c). Because this high rate of area-normalized production coincided with the annual peak in open water area, annual production in 2001 was among the highest of any year during the POI (Figure 8a), even though open water area was below average (Figure 3a). On the other hand, high rates of area-normalized production in May–June do not necessarily translate into high annual area-integrated production. For example, in 2003, a high daily rate of area-normalized production during May led to high total production during this month (Figure 7d), but the annual production was still relatively low (Figure 8a) because of depressed August–September values (Figure 7c). In 2006, the relatively high open water conditions earlier in the year (Figure 4a), coupled with a high area-normalized primary production rate (Figure 7c), led to high total production throughout the productive period of the year (Figure 8b), and therefore the highest annual production (Figure 8a) during the POI.

[34] Annual pan-Arctic primary production averaged 419 ± 33 Tg C a^{-1} during 1998–2006 (Figure 8a), with an interannual variability of 26% [(max − min)/mean]. Annual production peaked in 2006 at 483 Tg C a^{-1} and was lowest in 1998 at 375 Tg C a^{-1}. Overall, total Arctic primary production increased during 1998–2006, but not significantly ($R^2 = 0.4$, $p = 0.07$), increasing each year by an additional 7.62 Tg C a^{-1}. The relatively low coefficient of determination (R^2) between annual primary production and year is due to a period of decreased production between 2001 and 2003. This transient decrease in annual production is largely attributable to a drop in productivity during the months of August–September between 2001 and 2004 (Figure 8c). While total production during the two months of the spring bloom (May–June) (Figure 8b) exhibited a markedly increasing temporal trend, rising at the rate of 4.57 Tg C $a^{-1}\ a^{-1}$ ($R^2 = 0.6$, $p = 0.01$), there was no significant interannual trend in production during the period of maximum open water area (August–September) (Figure 8c).

3.2.2. Geographic Sectors

[35] Annual primary production in the Arctic varied widely between geographic sectors (Figure 9). The two largest sectors, the Greenland and Barents, also were the most productive (Figures 9e and 9f), averaging ~133 Tg C a^{-1} and 108 Tg C a^{-1}, respectively. Even though the Greenland and Barents sectors did not have the highest area-normalized production rate, the large seasonal and perennial open water area in these regions (Figure 5) resulted in high total annual production. Most of the other geographic sectors exhibited much lower rates of annual production during the POI,

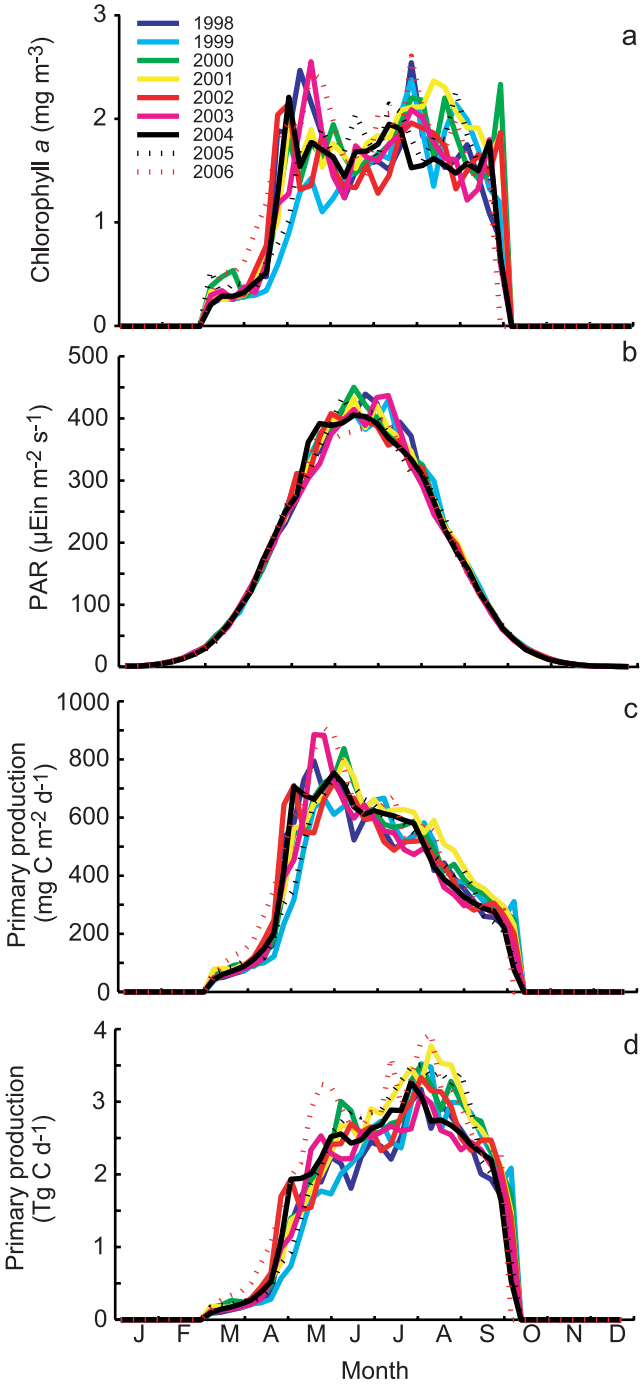

Figure 7. Weekly changes in (a) mean surface Chl *a* concentration, (b) mean daily photosynthetically active radiation (PAR) incident at the sea surface, (c) mean area-normalized daily primary production, and (d) annual primary production in the Arctic Ocean during 1998–2006.

generally in the range of 25–50 Tg C a^{-1}. Annual production was lowest in the Siberian sector, which averaged only ~17.8 Tg C a^{-1} during the POI (Figure 9i).

[36] The degree of interannual variability in annual primary production also was quite high between sectors (Figure 9). The Greenland sector exhibited the least amount of variability (Figure 9e), as determined from its low coefficient of variation (CV = standard deviation/mean) of 0.05. The Baffin, Barents, and Chukchi sectors exhibited an intermediate amount of interannual variability, with CVs for annual primary production all ranging from 0.10 to 0.15. The highest amount of interannual variability was observed in the Beaufort, Kara, Laptev, and Siberian sectors, which had CVs in the range of 0.24–0.29. In most sectors, yearly changes in annual primary production (Figure 9) can be explained by interannual changes in sea ice cover (Figure 5), with most geographic sectors exhibiting a significant correlation between these two quantities (Table 2). In fact, the sectors with the highest correlation between annual production and open water area (Beaufort, Barents, Kara, Laptev, and Siberian) were also the sectors with the highest degree of interannual variability in annual primary production. The unusually slight variation in annual production in the Greenland sector and the lack of a relationship with open water area was most likely due to the presence of a large area of permanently open water that varied little interannually.

[37] The Siberian was the only Arctic sector that exhibited a significant increase in annual primary production during the POI ($R^2 = 0.6, p = 0.009$), rising each year at the rate of 1.7 Tg C a^{-1} (Table 3). Most other sectors displayed either no obvious temporal trend between 1998 and 2006 or a slight, but nonsignificant increase (Figure 9). The Beaufort was the only sector where annual production actually decreased during the POI, falling each year at a rate of 1.5 Tg C a^{-1} ($R^2 = 0.4$, $p = 0.059$). However, this negative trend was not

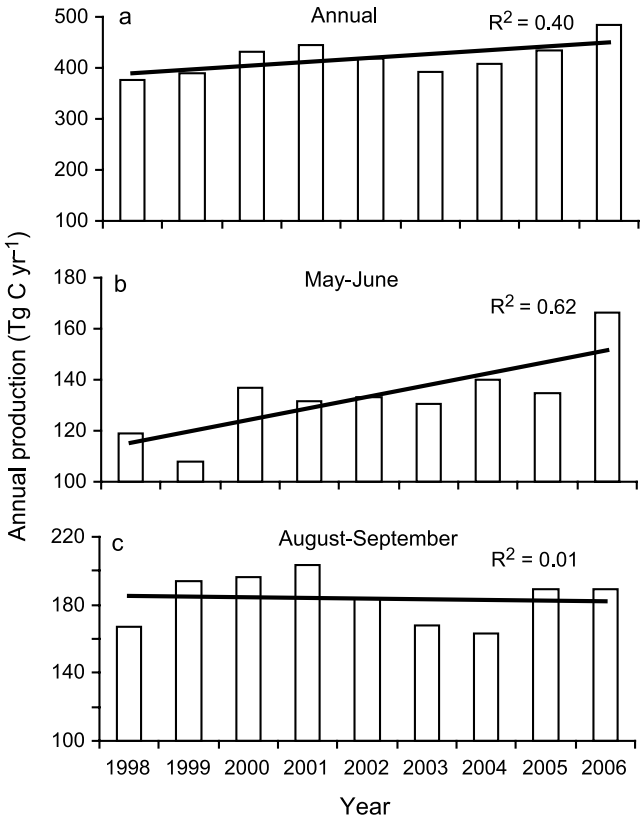

Figure 8. Total primary production computed for (a) the entire year, (b) the months of May–June, and (c) the months of August–September. Also shown is the long-term trend in primary production.

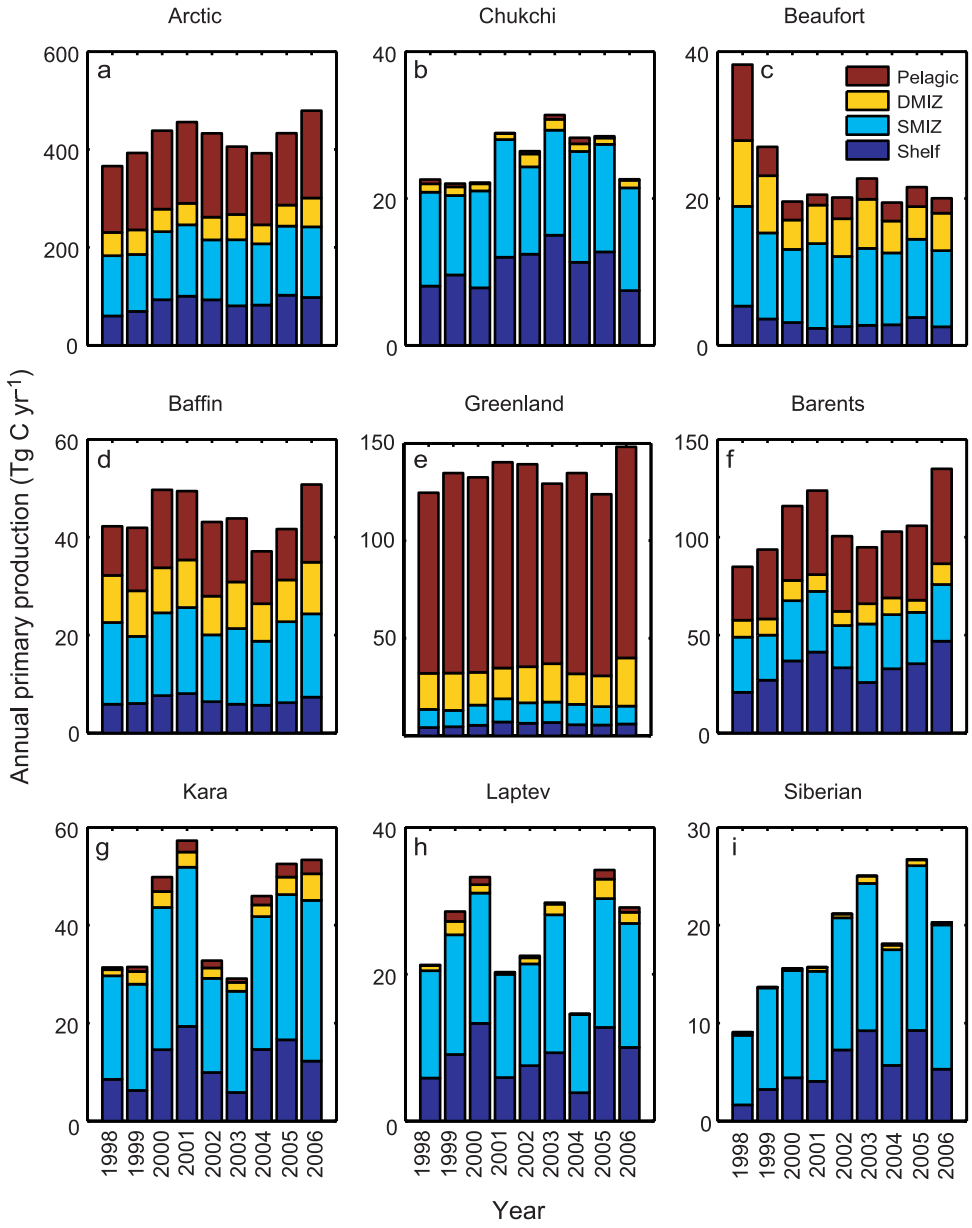

Figure 9. Annual primary production in the Arctic Ocean for each ecological province and geographical sector during 1998–2006.

statistically significant, being driven primarily by large decreases in production during the first 2 years of the POI (Figure 9). Between 2000 and 2006, annual production in the Beaufort remained relatively constant.

3.2.3. Ecological Provinces

3.2.3.1. Pelagic

[38] Among the ecological provinces of the Arctic, total annual production was highest in the pelagic province (Figure 9a), averaging 154 ± 13 Tg C a^{-1} during the POI, which constituted 34–40% of pan-Arctic annual primary production. The high annual production in this province is due to its large open water area, accounting for ~52% of the average open water area in the entire Arctic basin over a year. The pelagic province was the dominant contributor to annual production in the Greenland and the Barents sectors (Figures 9e and 9f), where it accounted for 75% (98 Tg C a^{-1}) and 35% (37 Tg C a^{-1}), respectively, of total annual production. There was no significant temporal trend in

Table 2. Linear Regression of Annual Primary Production Against Open Water Area by Geographic Sector[a]

	Chukchi	Beaufort	Baffin	Greenland	Barents	Kara	Laptev	Siberian	Arctic
Slope*	5.33	**9.17**	6.75	9.84	**13.4**	**12.7**	**12.4**	**11.3**	**12.1**
R^2	0.269	**0.895**	0.24	0.15	**0.866**	**0.893**	**0.896**	**0.942**	**0.617**
p Value	0.153	**<0.001**	0.181	0.304	**<0.001**	**<0.001**	**<0.001**	**<0.001**	**0.012**

[a]Slopes are in units of (10^7 g C a^{-1}) km^{-2}. Bolding denotes statistical significance at the 95% confidence level.

Table 3. Linear Regression of Annual Primary Production Against Year by Geographic Sector and Ecological Province[a]

	Chukchi	Beaufort	Baffin	Greenland	Barents	Kara	Laptev	Siberian	Arctic
				Shelf					
Slope	0.280	−0.183	0.000	0.170	1.783	0.539	0.204	**0.673**	3.466
R^2	0.087	0.278	0.000	0.220	0.365	0.099	0.031	**0.500**	0.438
p Value	0.442	0.145	0.998	0.203	0.085	0.409	0.650	**0.033**	0.052
				SMIZ					
Slope	0.308	−0.289	0.002	0.041	0.077	0.917	0.057	**0.924**	2.038
R^2	0.266	0.397	0.000	0.011	0.004	0.220	0.004	**0.738**	0.205
p Value	0.155	0.069	0.992	0.788	0.870	0.203	0.875	**0.003**	0.221
				DMIZ					
Slope	−0.009	−0.389	−0.029	0.314	−0.005	0.281	0.078	0.038	0.278
R^2	0.007	0.390	0.008	0.080	0.000	0.399	0.070	0.245	0.016
p Value	0.833	0.072	0.822	0.460	0.980	0.068	0.491	0.175	0.747
				Pelagic					
Slope	−0.010	−0.593	0.071	0.592	1.173	0.178	0.000	0.007	1.417
R^2	0.012	0.373	0.007	0.054	0.239	0.268	0.000	0.141	0.080
p Value	0.781	0.081	0.830	0.549	0.182	0.153	0.999	0.319	0.461
				Total					
Slope	0.576	−1.445	0.076	1.188	3.066	1.938	0.352	**1.648**	7.892
R^2	0.193	0.421	0.002	0.122	0.279	0.218	0.021	**0.647**	0.334
p Value	0.237	0.059	0.906	0.357	0.144	0.205	0.709	**0.009**	0.103

[a]Slopes are in units of (Tg C a^{-1}) a^{-1}. Bolding denotes statistical significance at the 95% confidence level.

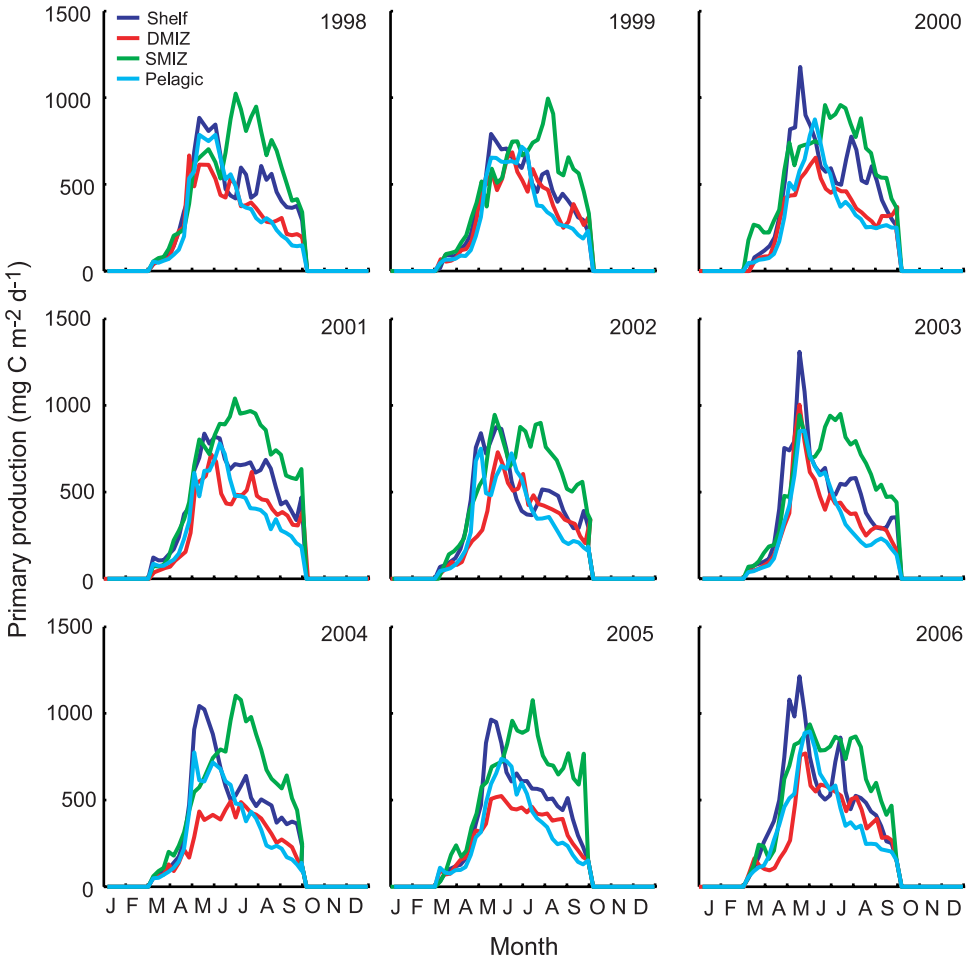

Figure 10. Weekly changes in daily area-normalized primary production in each ecological province of the Arctic Ocean during 1998–2006.

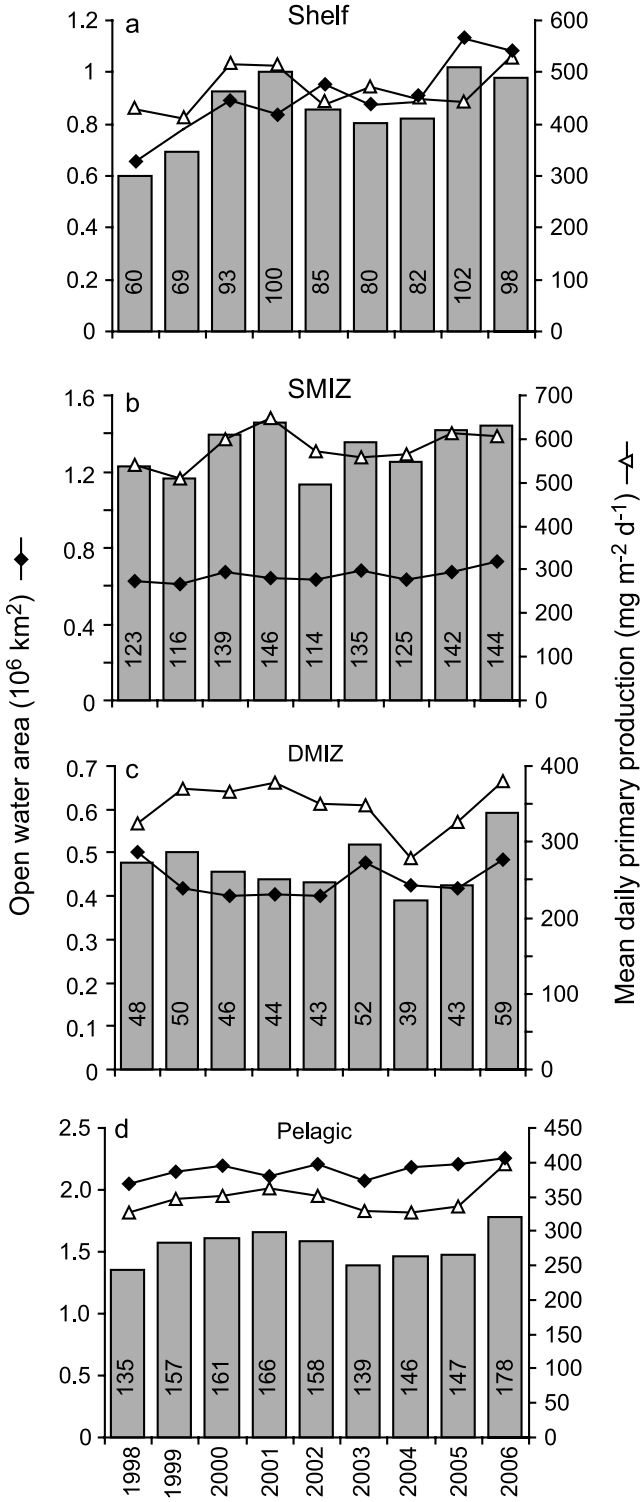

Figure 11. Total annual primary production (gray columns, given in Tg C a^{-1}), annual mean open water area and annual mean area-normalized primary production in the (a) shelf, (b) SMIZ, (c) DMIZ, and (d) pelagic provinces of the Arctic Ocean during 1998–2006.

annual production in the pelagic province, either for the entire Arctic Ocean or within individual geographic sectors. The area-normalized production rate in the pelagic province was lower than that of the shelf and the SMIZ provinces (Figure 10), averaging 348 ± 22 mg C m^{-2} d^{-1}, and exhibiting no interannual trend during the POI. The area-normalized production rate in the pelagic province reached its yearly maximum of 781–1016 mg C m^{-2} d^{-1} between April and mid-July (Figure 10).

3.2.3.2. Shelf

[39] Annual primary production in the shelf province averaged 86 ± 14 Tg C a^{-1} during the POI (Figure 9a), contributing 16–24% of pan-Arctic production. The shelf province was particularly important in the Barents, Kara, and Chukchi sectors (Figure 9), where it accounted for 31% (33 ± 8 Tg C a^{-1}), 32% (12 ± 4 Tg C a^{-1}), and 41% (10 ± 2 Tg C a^{-1}), respectively, of annual primary production in these sectors.

[40] The shelf exhibited the largest temporal increase in annual production of all the ecological provinces over the POI (R^2 = 0.44, p = 0.052), increasing each year by an average of 3.5 Tg C a^{-1} (Figure 11a). Although the 9-year trend was not statistically significant, increases in primary production were particularly dramatic for the last 2 years of the POI, exceeding 1998 levels by 70% and 63%, respectively, in 2005 and 2006. This increase was primarily due to a large and statistically significant (Table 1) increase in open water area in this province but also to a smaller (but not significant) increase in the daily area-normalized rate of production (Figure 11a). Open water area in the shelf province increased from 0.66 × 10^6 km^2 in 1998 to 1.13 × 10^6 km^2 (in 2005) and 1.09 × 10^6 km^2 (in 2006), an increase of 71% and 64%, respectively. In contrast, the area-normalized production rate increased by 3.5% in 2005 and 24% in 2006, relative to the 1998 value. The area-normalized rate of production in the shelf province during the spring bloom was the highest of all the other ecological provinces, ranging from 790 to 1308 mg C m^{-2} d^{-1} (Figure 10).

3.2.3.3. SMIZ

[41] Total annual production in the SMIZ was the second largest of all the ecological provinces (Figure 9a) and was comparable to that in the pelagic province, averaging 132 ± 6.0 Tg C a^{-1} during the POI and representing 28–33% of the Arctic Ocean annual primary production. This was despite the fact that the SMIZ comprised on average only ~16% of the open water in the Arctic Ocean over a year. There was no significant interannual trend for total annual production in the SMIZ over the POI (R^2 = 0.2, p = 0.21, Table 3). The SMIZ province was particularly important in the Kara, Laptev and Siberian sectors, where it contributed >60% (>15 Tg C a^{-1}) of annual primary production (Figure 9). The SMIZ was the dominant province in the Chukchi, Beaufort, and Baffin sectors as well, accounting for 53% (14 Tg C a^{-1}), 48% (10 Tg C a^{-1}), and 35% (16 Tg C a^{-1}) of sector-wide production, respectively.

[42] The high total annual production in the SMIZ resulted from an area-normalized production rate that was higher than in any other ecological province, averaging 579 ± 42 mg C m^{-2} d^{-1} over the POI and reaching as high as 982–1174 mg C m^{-2} d^{-1} during the peak of the spring bloom (Figure 10). The dominance of the SMIZ persisted

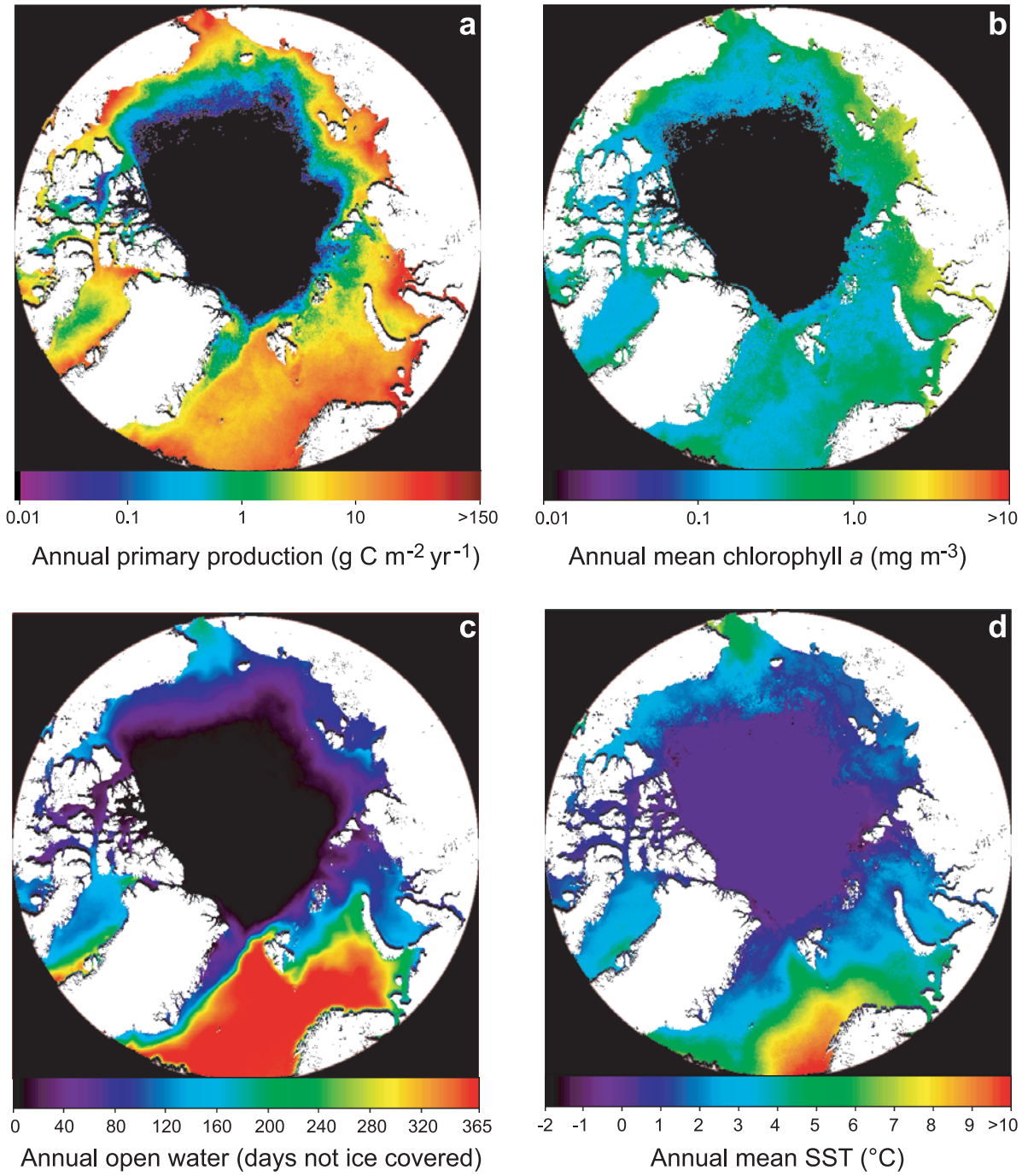

Figure 12. Climatologies (1998–2006) for (a) annual primary production, (b) annual mean surface Chl *a*, (c) annual mean open water (number of ice-free days per year), and (d) annual mean sea surface temperature.

for most of the year, except during April–May when it was eclipsed by the daily production rate in the shelf province. The area-normalized production rate was highest in 2001 and 2006, averaging 650 and 606 mg C m^{-2} d^{-1}, respectively.

3.2.3.4. DMIZ

[43] Annual production in the DMIZ was the lowest of all the ecological provinces (Figure 9) and displayed no significant temporal trend during the POI (Table 3). With annual production rates averaging 47 ± 12 Tg C a^{-1} (Figure 9a), the DMIZ contributed just 9.6–13% of annual primary production in the Arctic Ocean. This low value was due more to a small amount of open water area in this province than to low area-normalized production rates, which were similar to those in the pelagic province, averaging 347 ± 32 mg m^{-2} d^{-1} over the POI. Rates of area-normalized production were highest in 2001 and 2006, exhibiting values of 377 and 379 mg m^{-2} d^{-1}, respectively (Figure 10).

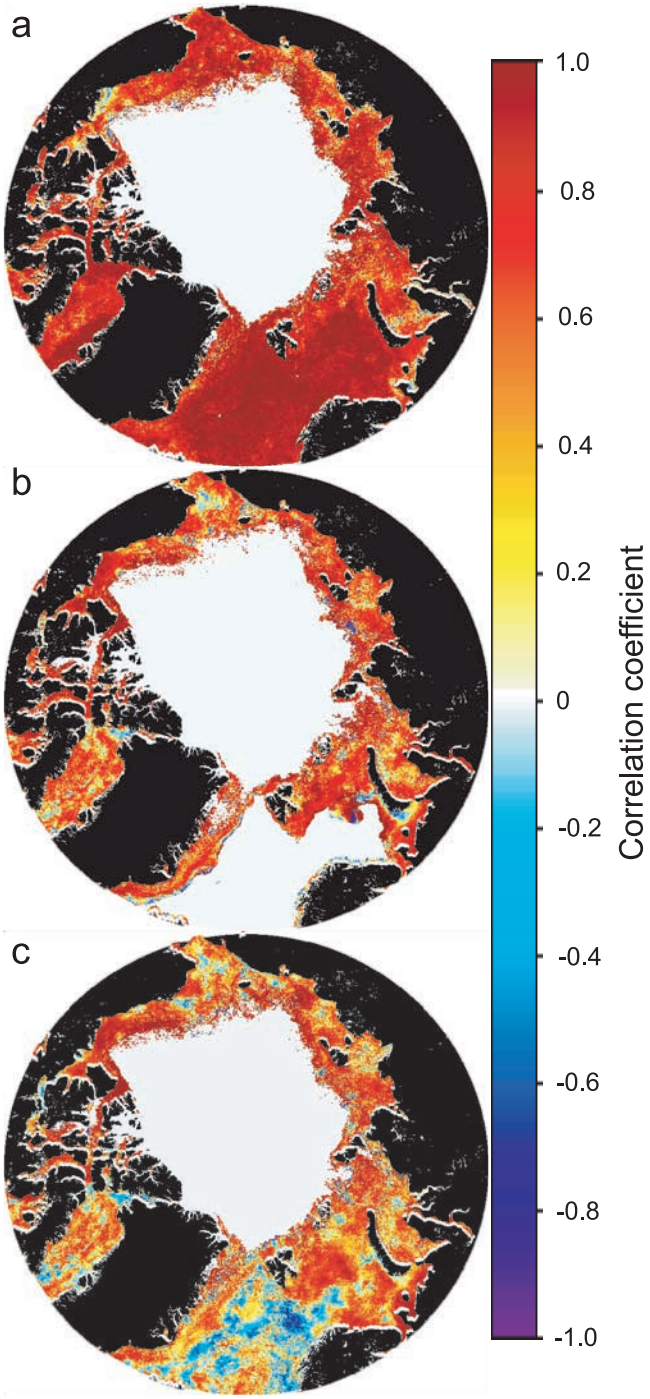

Figure 13. Maps of the correlation coefficient for the regression of annual mean primary production against (a) annual mean surface Chl *a*, (b) annual mean open water area (only in regions where open water is present for ≤350 days), and (c) annual mean sea surface temperature for the 9 years of our study. Only pixel locations where data are available for all 9 years are shown in color.

[44] The DMIZ province was most productive in the Greenland sector (Figure 9), contributing 18 Tg C a^{-1} or 14% of total annual production in this sector. Although the DMIZ accounts for a higher proportion of annual production in the Beaufort (25%) and Baffin (21%) sectors, total DMIZ production there (5 and 9 Tg C a^{-1}, respectively) was considerably less than in the Greenland sector.

3.2.3.5. Total Shelves

[45] Despite accounting for only 30–40% of total open water area, the combined annual production of the two provinces associated with the shallow waters of continental shelf, the shelf and SMIZ provinces, contributed the majority of annual primary production in the Arctic (Figure 9). Over the entire Arctic Ocean, the annual mean production in the waters of the shelf and SMIZ combined (217 Tg C a^{-1}) exceeded the production of the offshore waters of the pelagic and the DMIZ provinces (201 Tg C a^{-1}). Primary production on the continental shelves was particularly important in the Chukchi, Siberian, Laptev, and Kara sectors, where the SMIZ + shelf accounted for 90% or more of annual production.

3.2.4. Controls of Primary Production

[46] In general, the spatial pattern of annual primary production (Figure 12a) most closely mimics that of Chl *a* over most of the Arctic Ocean (Figure 12b). Of course the high correlation between primary production and Chl *a* concentration (Figure 13a) is to be expected, given that our algorithm computes primary production from Chl *a* and an estimate of the phytoplankton growth rate (equation (2)). While SST also plays an important role, the large amount of spatial and temporal variability exhibited by Chl *a*, which can range over 4 orders of magnitude, far outweighs the relatively smaller variability characteristic of SST. For example, primary production anomalies (Figure 14), calculated as the difference between the annual mean for a single year and the 9-year mean (Figure 12a), are largest (±80 g C m^{-2} a^{-1}) in waters with high Chl *a* variability (Figure 15).

[47] Because phytoplankton blooms require ice-free surface waters in order to obtain sufficient light for net growth, primary production also is positively correlated with open water area in most sectors of the Arctic Ocean (Figure 13b). The higher rates of primary production in the Arctic in recent years are reflected in large and widespread positive primary production anomalies, particularly in 2005 and 2006 (Figure 14), that correspond to strong positive open water anomalies (Figure 16). In 2006, annual primary production was >60 g C m^{-2} a^{-1} higher than the 9-year average (Figure 12a) in some parts of the Barents, Kara, and Greenland sectors. While anomalously high rates of production in 2005 and 2006 were due in part to unusually high Chl *a* concentrations (Figure 15), open water conditions in some regions persisted for >150 days longer than average (Figure 16), greatly extended the length of the phytoplankton growing season. In the Siberian sector, where open water area increased significantly during the POI, the changes in production also were positive, although modest (20–40 g C m^{-2} a^{-1}), especially since 2002. This increase resulted from both higher Chl *a* concentrations and open water area in these waters after 2003. The negative primary production anomalies (<–60 g C m^{-2} a^{-1}) in the Barents and Kara sectors in 2003 were mainly due to anomalously low Chl *a* concentrations, since open water area in these regions differed little from other years.

[48] Primary production was positively correlated with SST (Figure 13c) in all sectors except the Greenland. The positive correlation of SST with primary production is due

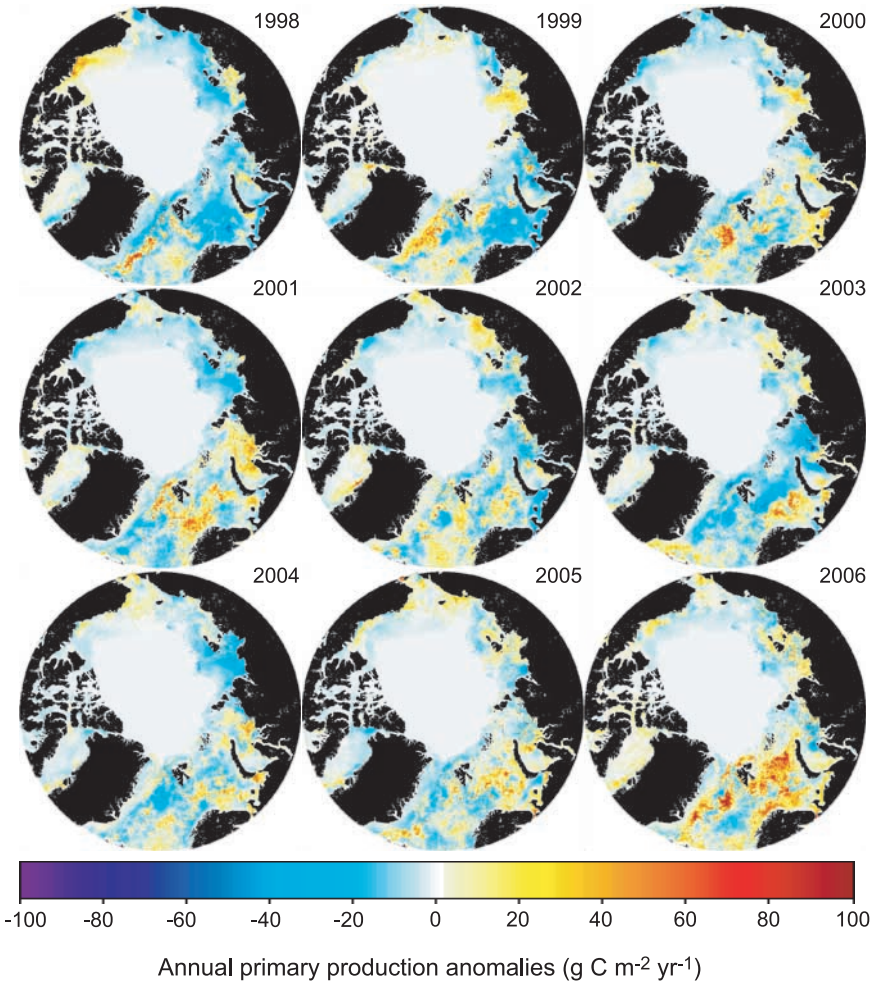

Figure 14. Anomaly maps of annual primary production for each of the 9 years of this study. Colors represent change from the climatological mean shown in Figure 12a.

both to direct effects of SST on phytoplankton growth rates (equation (2)) and indirect effects of SST on surface water stratification, impacting both light and nutrient availability. It is interesting to note that the correlation between SST and annual primary production (Figure 13c) is spatially similar to the correlation between open water area and annual primary production (Figure 13b), indicating that the correlation between the SST and open water area is also high.

4. Discussion

4.1. Comparison With Previous Results

[49] Unfortunately, there are very few historical estimates of pan-Arctic primary production with which to compare our results. *Subba Rao and Platt* [1984] estimated that the annual rate of Arctic-wide primary production for all waters north of 65°N was 206 Tg C a^{-1}, approximately half the mean value estimated here (419 Tg C a^{-1}). Because the study region used by *Subba Rao and Platt* [1984] was slightly larger area than that used here, the primary reason for the discrepancy between the two values is that their estimate of mean area-normalized production for the Arctic (9–27 g C m^{-2} a^{-1}) was considerably lower than ours (44 g C m^{-2} a^{-1}). However, our value is in much better agreement with the much more recent pan-Arctic productivity estimate of 329 Tg C a^{-1} made by *Sakshaug* [2003], which was based on a compilation of both historical measurements and model results. The computed annual primary production in the early years of our study is within 10% of the estimate of *Sakshaug* [2003]. This early period should bear a greater similarity to the historical observations compiled by *Sakshaug* [2003], which were made prior to the rapid increase in open water area observed recently. In later years (e.g., 2006), our estimate of production is 50% higher than that of *Sakshaug* [2003], due mostly to the dramatic increases in open water area but also to the slight increase in daily area-normalized production rates.

[50] Annual rates of primary production computed here are likely to be underestimates of actual rates because insufficient spatial resolution of satellite data, make it impossible to quantify primary production in the leads and melt ponds within the Arctic sea ice zone that are known sinks for atmospheric CO_2 [*Semiletov et al.*, 2004]. Furthermore, the primary production algorithm does not account for production by phytoplankton growing under sea ice and by sea ice algae, although this is likely to represent only a small fraction of total Arctic primary production. Most importantly, calculated rates of primary production in

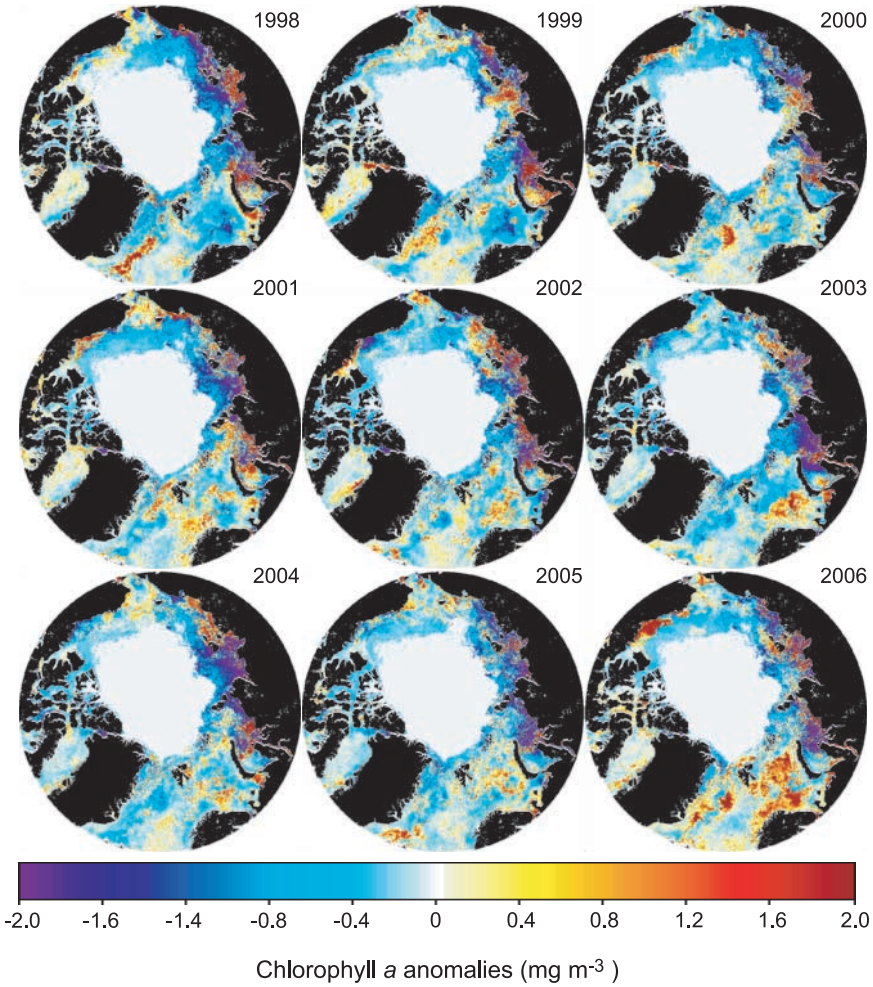

Figure 15. Anomaly maps of surface Chl *a* for each of the 9 years of this study. Colors represent change from the climatological mean shown in Figure 12b.

the summer may be low because of the subsurface chlorophyll maximum (SCM) that occasionally develops offshore and is unresolved by SeaWiFS [*Falk-Petersen et al.*, 2000; *Hill and Cota*, 2005; *Matrai et al.*, 2007]. In some areas, productivity is highest at the ocean surface despite the presence of a SCM [e.g., *Matrai et al.*, 2007], suggesting that these SCMs were the result of an increase in phytoplankton Chl *a* per cell with depth, rather than an actual subsurface peak in phytoplankton abundance. In these waters, our algorithm should still work quite well. However, in those situations where the depth of the SCM corresponds to the depth of the productivity peak [e.g., *Hill and Cota*, 2005], depth-integrated water column production calculated by our algorithm is well below the in situ estimate. For example, *Hill and Cota* [2005] observed numerous stations with a SCM in the western Arctic. Surface Chl *a* at these stations averaged 0.4 mg m^{-3}, while the Chl *a* concentration at the depth of the SCM averaged 2.5 mg m^{-3}. The depth-integrated primary production for these stations averaged approximately 600 mg C m^{-2} d^{-1}, well above the range of values produced by our algorithm for a surface Chl *a* concentration of 0.4 mg m^{-3} (Figure 2b). The prevalence of subsurface productivity maxima missed by SeaWiFS and their impact on annual primary production estimates is unclear. Approximately 25% of the July–August stations shown in Figure 2b exhibited a significant subsurface productivity maximum that was not accounted for by our algorithm. Given that July and August account for approximately 40% of annual primary production (Figure 7d), if our algorithm underestimated primary production over 25% of the Arctic Ocean during these two months by as much as a factor of two, then the actual annual production would be only 10% higher than we have estimated here.

4.2. Temporal Changes in Primary Production

[51] Between 1998 and 2006, annual primary production in the Arctic Ocean increased by ~30%, in sharp contrast to lower latitudes where primary production appears to have declined in recent years [*Behrenfeld et al.*, 2006]. Changes in primary production in the Arctic also differed markedly from trends observed in the Southern Ocean, where rates of annual production between 1997 and 2006 were ~fivefold higher than those estimated here, but with much less interannual variability (11% versus 26% for the Arctic) and no significant temporal trend.

[52] However, the change in annual primary production in the Arctic between 1998 and 2006 was not monotonic (Figure 8a), increasing in the early years of the POI

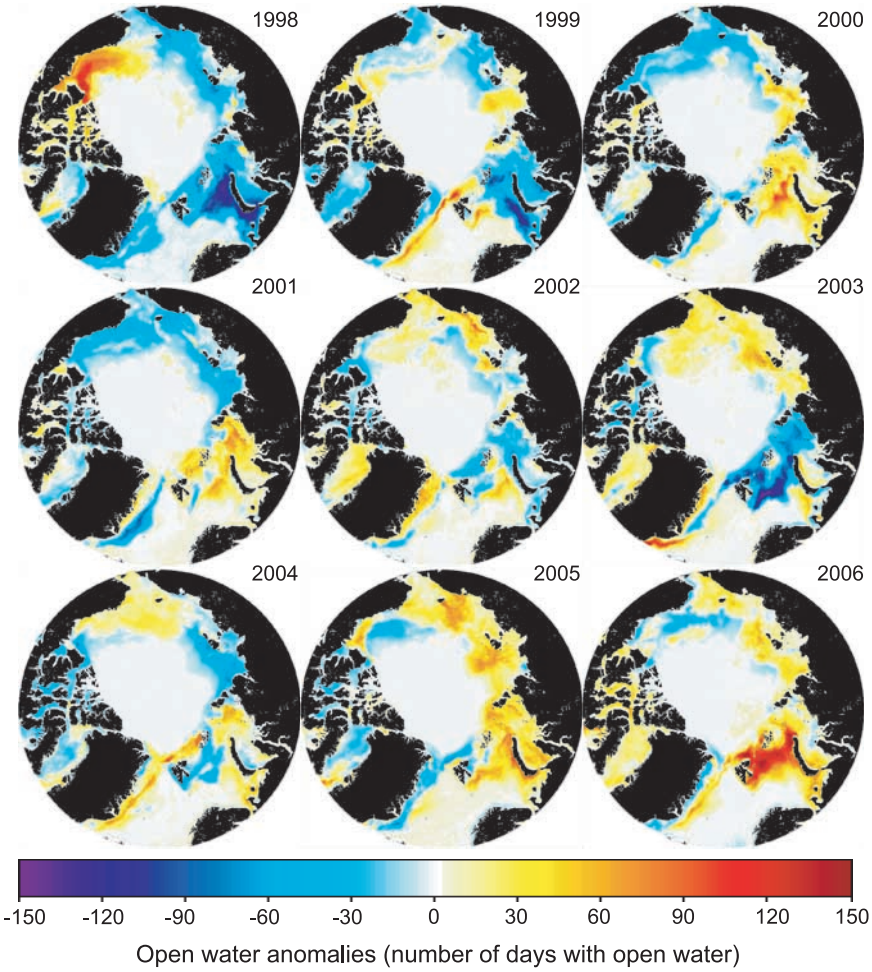

Figure 16. Anomaly maps of open water area for each of the 9 years of our study. Colors represent change from the climatological mean shown in Figure 12c.

(1998–2001), decreasing thereafter until 2003, and then rising again to the maximum value attained during the POI in 2006 (483 Tg C a^{-1}). Because of this irregular temporal pattern, the secular trend in annual primary production was not statistically significant ($R^2 = 0.4$, $p = 0.07$). In contrast, the amount of open water area, which is a major factor controlling annual primary production, did exhibit a statistically significant increase between 1998 and 2006 (Figure 3a). This difference suggests that the temporal trends observed in primary production were driven in large part by interannual changes in the rate of area-normalized production, rather than by changes in sea ice extent. For example, the local maximum in annual primary production in 2001 was the result of both higher than normal phytoplankton biomass and higher area-normalized rates of production during the late summer bloom of that year, despite open water area being relatively low (Figure 3a). The cause for this increase can clearly be seen by closer inspection of the primary production anomaly in 2001 (Figure 14), which shows that elevated production in the Barents and Kara sectors coincided with a highly positive Chl *a* anomaly in these regions (Figure 15), but with no discernable changes in the open water area (Figure 16) or SST (Figure 17). Similarly, the drop in annual production between 2001 and 2003, despite a slight increase in open water area, was closely tied to a coincident drop in area-normalized production in all four of the ecological provinces in the Arctic Ocean (Figure 11). Thus, changes in total production in the Arctic were not simply a consequence of increased open water area in recent years; changes in phytoplankton biomass and area-normalized production also played important roles. This was especially true in 2005 and 2006 when both the area-normalized rate of production and open water area were at or near their 9-year highs, elevating 2006 to the most productive year of the POI.

[53] Although the precise cause of the observed interannual variation in area-normalized production is not clear, changes taking place in the Greenland Sea, particularly from 2004 to 2006, may provide some clues. Over most of the Arctic, we observed a strong positive correlation between annual mean SST and annual primary production (Figure 13c). The major exception to this pattern is found in those parts of the Greenland Sea that remain ice free all year (red areas in Figure 12c). In these waters, positive SST anomalies (Figure 17) coincided with negative primary production anomalies (Figure 14), resulting in an atypical negative correlation between SST and annual primary production (Figure 13c). The temperature of these waters

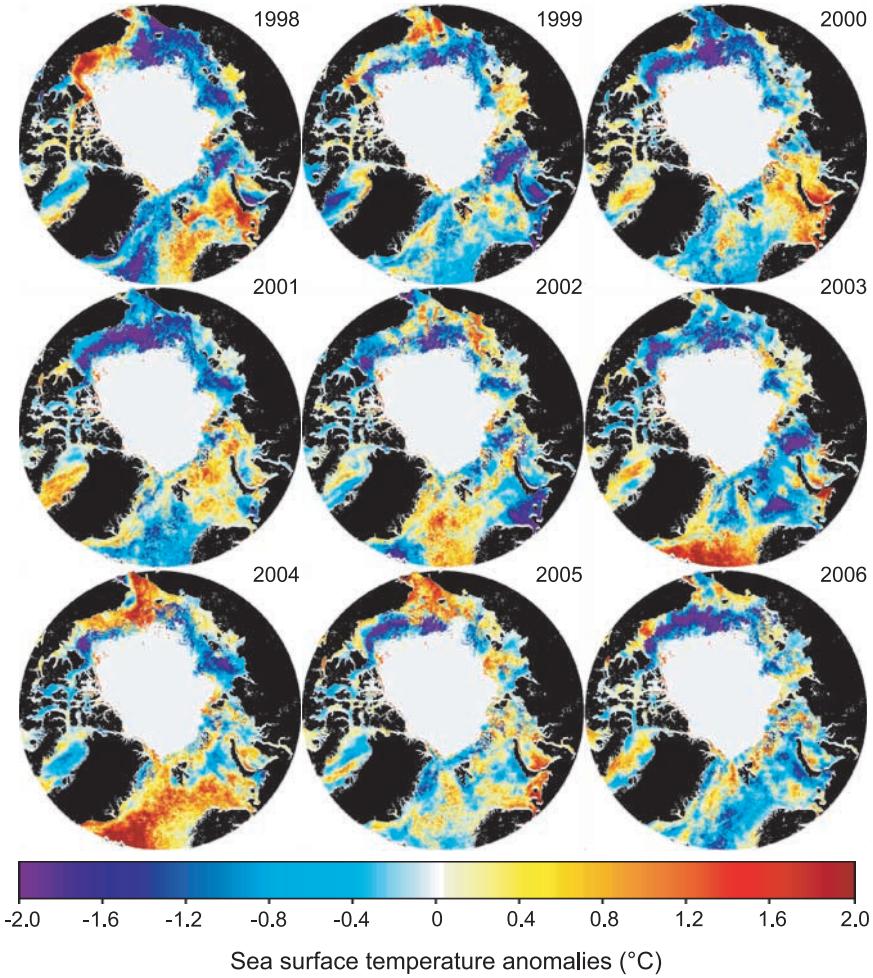

Figure 17. Anomaly maps of sea surface temperature for each of the 9 years of our study. Colors represent change from the climatological mean shown in Figure 12d.

is known to be especially sensitive to the phase of the Arctic Oscillation (AO) [*Wanner et al.*, 2001]. As the AO becomes more positive, westerly winds strengthen, northward advection of North Atlantic waters increases, and waters in the western Greenland Sea cool [*Thompson and Wallace*, 1998]. As can be seen in our study, a cooler Greenland Sea is associated with enhanced Chl *a* concentrations in these waters and positive annual primary production anomalies. This pattern is particularly evident from 2004 through 2006, when cooling of the open waters of the Greenland Sea (Figure 17) was associated with a marked increase in both Chl *a* (Figure 16) and primary production (Figure 14). Although the mechanism behind the elevated production in a cooler Greenland Sea is not presently known, the increased northward advection of North Atlantic water during positive phases of the AO may enhance the flux of nutrients into the Greenland Sea that stimulate the growth of phytoplankton and increase annual primary productivity.

[54] It should be noted, however, that the temporal pattern of annual pan-Arctic primary production was not well correlated with the AO index (data from the NOAA climate monitoring center, http://www.cpc.ncep.noaa.gov/products/precip/CWlink/daily_ao_index/ao_index.html), averaged either annually (R^2 = 0.016, p = 0.74) or only over the more critical winter months (November–April, R^2 = 0.013, p = 0.77). However, the AO is most highly correlated with annual primary production in the Greenland Sea, by far the most productive sector of the Arctic Ocean (Figure 9), although even there it explains only 29% of the interannual variability (p = 0.12) between 1998 and 2006. This lends support to the notion that increased advection of waters into the Greenland Sea during a positive phase of the AO could play an important role in enhancing phytoplankton productivity. It must be remembered, however, that the AO is complex and does not actually exist in two quasi-stable states (positive or negative), as was suggested by the simple description given above. Instead, the AO is highly dynamic and can vary markedly on monthly timescales. Thus, it is not surprising that the correlation between annual primary production and the AO is relatively weak, even in the Greenland Sea where its impacts are expected to be most apparent.

4.3. Recent Loss of Sea Ice

[55] The results presented in this study show that during 1998–2006, the loss of sea ice (and increase in open water area) was not uniform across the Arctic, being more pronounced in some geographic sectors than in others. Open water area increased most rapidly in the Barents and

Kara sectors, and most significantly in the Siberian sector. The observed decrease in sea ice in these sectors is consistent with the previously documented decreasing trend in ice thickness between 1987 and 1999 by *Rothrock et al.* [2003]. The dramatic loss of sea ice in the Siberian sector is particularly alarming because model results demonstrate that changes in the Siberian Sea can be a precursor to basin-wide changes in sea ice thickness [*Rothrock et al.*, 2003; *Ukita et al.*, 2007]. Our study shows that the rate of loss of sea ice in these waters has been accelerating in recent years, particularly since 2003.

[56] The accelerated changes of sea ice extent and thickness in the Arctic are due to multiple factors. Foremost is the loss of ice due to wind stress changes that increase the advection of sea ice out of the Arctic [*Zhang et al.*, 2000; *Holloway and Sou*, 2002]. This impact can be amplified by increased melting and a longer melt season, resulting in a positive feedback on sea ice loss [*Smith*, 1998; *Laxon et al.*, 2003]. The rate of sea ice melt also may be accelerated by the observed increase in water temperature in recent years. This temperature increase has been attributed to a combination of warmer Pacific waters entering through the Bering Strait [*Fukasawa et al.*, 2004; *Shimada et al.*, 2006] and a rise in downward longwave radiation [*Francis and Hunter*, 2006] resulting from an increase in liquid-water clouds relative to ice clouds [*Zuidema et al.*, 2005; *Francis and Hunter*, 2006]. Consistent with this viewpoint, *Serreze et al.* [2003] suggested that the recent changes in Arctic sea ice cover, particularly the low sea ice extent in 2002, were due to increased advection of heat into the Arctic Ocean during spring, coupled with high temperature and low pressure in summer that was affected by the cyclogenesis along northeastern Eurasia. In contrast, *Rigor et al.* [2002] and *Rigor and Wallace* [2004] argue that anomalous changes in sea ice are due to winter wind anomalies associated with the high-index AO conditions that increase the advection of ice away from the Eurasian and Alaskan coasts. Regardless of the relative importance of meteorological conditions in the winter and spring, losses of Arctic ice have been extensive in recent years, exemplified by the dramatic 30% decrease between 2006 and 2007 in the extent of perennial sea ice during the summer [*Comiso et al.*, 2008].

4.4. Other Environmental Changes in the Arctic

[57] Primary production in the Arctic is likely to vary in response to changes in a number of other environmental factors that influence the onset and development of phytoplankton blooms, including PAR at the upper ocean surface, nutrient inventories, and freshwater content. For example, mean Arctic-wide PAR exhibited a slow but steady decrease during the POI, dropping each year by an average of 0.7 μEin m^{-2} s^{-1} (R^2 = 0.74). PAR was highest in 1999 (annual mean of 201 μEin m^{-2} s^{-1}) and lowest in 2006 (annual mean of 195 μEin m^{-2} s^{-1}). Using our primary production algorithm, we calculate that the observed 3% decrease in PAR between 1999 and 2006 should translate into in a 1% decrease in annual primary production.

[58] More importantly, there has been a significant rise in freshwater content in the Arctic due to melting of sea ice and glaciers, excess precipitation, and increasing river discharge [*Peterson et al.*, 2002]. The rise in river discharge is due primarily to increased runoff from Asian rivers, which currently adds 2560 km^3 of freshwater to the Arctic Ocean each year, an increase of 5% over the mean from the previous 20 years [*Richter-Menge et al.*, 2006]. Discharge from the Yukon and Mackenzie rivers in recent years also was higher than normal [*Richter-Menge et al.*, 2006], most likely due to an increase in net excess precipitation over evaporation (P-E) at high latitudes [*Peterson et al.*, 2002]. Enhanced melting of glaciers [*Dyurgerov and Carter*, 2004] and the Greenland ice sheet [*Box et al.*, 2004] further contributed to the recent increase in freshwater content of the Arctic. Finally, the contribution of freshwater from melting sea ice in the Arctic increased from 8000 km^3 in 1980 to 17,000 km^3 in 1997 [*Peterson et al.*, 2006]. These changes in Arctic freshwater input, especially from river runoff (which also contributes substantial amounts of sediment and organic matter), alter the availability of both nutrients and light necessary for phytoplankton growth. Increasing freshwater content intensifies surface stratification, thereby decreasing the thickness of the upper mixed layer, increasing light availability, and partially offsetting the drop in irradiance due to increased turbidity and decreases in incident PAR. On the other hand, increased stratification would likely reduce the supply of nutrients from the deeper waters beneath the mixed layer, decreasing phytoplankton growth and productivity.

[59] While increasing air temperature appears to have governed the processes of excess river discharge and accelerated sea ice melt in recent years, the P-E anomaly seems to be more closely tied to the changes in the AO [*Peterson et al.*, 2006]. *Steele and Ermold* [2004] report considerable freshening of the western Siberian shelf sea (White Sea and Kara Sea) and salinification of the eastern Siberian shelf seas. Fresh water tends to accumulate in the Arctic Ocean during the negative phase of the AO and subsequently exits to the North Atlantic during the positive AO phase [*Dickson*, 1999]. However, the poor correlation we report between the AO index and both phytoplankton biomass and primary production in the Arctic suggests that these oceanographic manifestations of the AO may be very localized or may operate on timescales or at times of year that reduce their impact on phytoplankton productivity in the Arctic. The AO seems to exert its greatest influence during the coldest part of the year (November–April), when low light conditions preclude phytoplankton growth. The extent to which stratification intensified by a negative AO persists into the spring and summer may ultimately determine its impact on rates of primary production.

4.5. Future Changes in Arctic Ocean Phytoplankton Productivity

[60] The increase in the flux of CO_2 from the atmosphere into the Arctic Ocean has tripled over the last 3 decades (from 24 to 66 Tg C a^{-1}) [*Bates et al.*, 2006]. This increase is attributed to the recent loss of sea ice that facilitated both increased primary production and sea-air CO_2 exchange. The recent increase in primary production reported here should further enhance this exchange, due to the reduction in surface water pCO_2 during the conversion of inorganic CO_2 to organic carbon by phytoplankton that eventually sinks below the thermocline. Although it has been calculated that outgassing of CO_2 will increase by 8 g C m^{-2} a^{-1}

for every 1°C increase in sea surface temperature [*Anderson and Kaltin*, 2001], the biologically mediated decrease in surface pCO_2 should partially offset the increased outgassing of CO_2 expected as Arctic surface waters warm in upcoming years. In fact, it has been suggested that when anticipated changes in CO_2 solubility (due to changes in both temperature and salinity) and phytoplankton production are taken into account, the potential for the Arctic Ocean to act as a sink for atmospheric CO_2 will increase in the future [*Anderson and Kaltin*, 2001]. However, longer-term observations are required to understand the extent to which primary production will be either intensified or weakened by the many concurrent environmental changes ongoing in the Arctic Ocean (e.g., declines in sea ice cover, increased SST, increased freshwater fluxes, changes in nutrient and light availability). In addition, although our study quantifies large-scale changes in the primary production of northern polar seas, it is unable to address any ongoing taxonomic changes within the phytoplankton community within the Arctic Ocean [*Booth and Horner*, 1997] as a consequence of observed environmental changes. Finally, further studies are required to quantify the extent to which the negative feedback between losses of sea ice and increased biological CO_2 uptake in the Arctic (which would reduce atmospheric warming) will be countered by the increased CO_2 outgassing resulting from surface ocean warming due to reduced sea ice albedo [*Morales-Maqueda et al.*, 1999]. This understanding is particularly critical given the unprecedented acceleration of sea ice loss observed in the Arctic in recent years.

[61] **Acknowledgments.** This research was supported by a NASA Earth Systems Science fellowship to S. Pabi (ESSF/04-0000-0293) and NASA grant NNG05GC92G to K. Arrigo. We would like to thank Jean-Eric Tremblay and the SBI investigators who made their data available for algorithm validation. We would like to thank Lindsey Kropuenske for comments on an earlier version of this manuscript.

References

Anderson, L. G., and S. Kaltin (2001), Carbon fluxes in the Arctic Ocean—Potential impact by climate change, *Polar Res.*, *20*(2), 225–232, doi:10.1111/j.1751-8369.2001.tb00060.x.

Arctic Climate Impact Assessment (2005), Arctic Climate Impact Assessment, scientific report, Cambridge Univ. Press, Cambridge, U. K.

Arrigo, K. R., and C. W. Sullivan (1994), A high resolution bio-optical model of microalgal growth: Tests using sea ice algal community time-series data, *Limnol. Oceanogr.*, *39*(3), 609–631.

Arrigo, K. R., D. Worthen, A. Schnell, and M. P. Lizotte (1998), Primary production in Southern Ocean waters, *J. Geophys. Res.*, *103*, 15,587–15,600, doi:10.1029/98JC00930.

Arrigo, K. R., G. L. van Dijken, and S. Bushinsky (2008), Primary production in the Southern Ocean, 1997–2006, *J. Geophys. Res.*, *113*, C08004, doi:10.1029/2007JC004551.

Bates, N. R., S. B. Moran, D. A. Hansell, and J. T. Mathis (2006), An increasing CO_2 sink in the Arctic Ocean due to sea ice loss, *Geophys. Res. Lett.*, *33*(23), L23609, doi:10.1029/2006GL027028.

Behrenfeld, M. J., R. T. O'Malley, D. A. Siegel, C. R. McClain, J. L. Sarmiento, G. C. Feldman, A. J. Milligan, P. G. Falkowski, R. M. Letelier, and E. S. Boss (2006), Climate-driven trends in contemporary ocean productivity, *Nature*, *444*(7120), 752–755, doi:10.1038/nature05317.

Boetius, A., and E. Damm (1998), Benthic oxygen uptake, hydrolytic potentials and microbial biomass at the Arctic continental slope, *Deep Sea Res. Part I*, *45*(2–3), 239–275, doi:10.1016/S0967-0637(97)00052-6.

Booth, B. C., and R. A. Horner (1997), Microalgae on the Arctic Ocean section, 1994: Species abundance and biomass, *Deep Sea Res, Part II*, *44*(8), 1607–1622, doi:10.1016/S0967-0645(97)00057-X.

Box, J. E., D. H. Bromwich, and L.-S. Bai (2004), Greenland ice sheet surface mass balance 1991–2000: Application of Polar MM5 mesoscale model and in situ data, *J. Geophys. Res.*, *109*, D16105, doi:10.1029/2003JD004451.

Buck, K. R., T. G. Nielsen, B. W. Hansen, D. Gastrup-Hansen, and H. A. Thomsen (1998), Infiltration phyto- and protozooplankton assemblages in the annual sea ice of Disko Island, West Greenland, spring 1996, *Polar Biol.*, *20*(6), 377–381, doi:10.1007/s003000050317.

Carmack, E. C., and R. W. Macdonald (2002), Oceanography of the Canadian shelf of the Beaufort Sea: A setting for marine life, *Arctic*, *55*, 29–45.

Carmack, E. C., K. Aagaard, J. H. Swift, R. W. Macdonald, F. A. McLaughlin, E. P. Jones, R. G. Perkin, J. N. Smith, K. M. Ellis, and L. R. Killius (1997), Changes in temperature and tracer distributions within the Arctic Ocean: Results from the 1994 Arctic Ocean section, *Deep Sea Res. Part II*, *44*(8), 1487–1502, doi:10.1016/S0967-0645(97)00056-8.

Cavalieri, D. J., C. L. Parkinson, and K. Y. Vinnikov (2003), 30-year satellite record reveals contrasting Arctic and Antarctic decadal sea ice variability, *Geophys. Res. Lett.*, *30*(18), 1970, doi:10.1029/2003GL018031.

Chapman, W. L., and J. E. Walsh (1993), Observed climate change in the Arctic, updated from Chapman and Walsh, 1993: Recent variations of sea ice and air temperatures in high latitudes, *Bull. Am. Meteorol. Soc.*, *74*(1), 33–47, doi:10.1175/1520-0477(1993)074<0033:RVOSIA>2.0.CO;2.

Codispoti, L. A. (1979), Arctic Ocean processes in relation to the dissolved silicon content of the Atlantic, *Mar. Sci. Commun.*, *5*(6), 361–381.

Comiso, J. C., C. L. Parkinson, R. Gersten, and L. Stock (2008), Accelerated decline in the Arctic sea ice cover, *Geophys. Res. Lett.*, *35*, L01703, doi:10.1029/2007GL031972.

Dickson, B. (1999), Oceanography: All change in the Arctic, *Nature*, *397*(6718), 389–391, doi:10.1038/17018.

Dyurgerov, M. B., and C. L. Carter (2004), Observational evidence of increases in freshwater inflow to the Arctic Ocean, *Arct. Antarct. Alp. Res.*, *36*(1), 117–122, doi:10.1657/1523-0430(2004)036[0117:OEOIIF]2.0.CO;2.

Eppley, R. W. (1972), Temperature and phytoplankton growth in the sea, *Fish. Bull.*, *70*(4), 1063–1085.

Falk-Petersen, S., H. Hop, W. Budgell, E. Hegseth, R. Korsnes, T. Loyning, J. Orbaek, T. Kawamura, and K. Shirasawa (2000), Physical and ecological processes in the marginal ice zone of the northern Barents Sea during the summer melt period, *J. Mar. Syst.*, *27*(1–3), 131–159, doi:10.1016/S0924-7963(00)00064-6.

Francis, J. A., and E. Hunter (2006), New insight into the disappearing Arctic sea ice, *Eos Trans. AGU*, *87*(46), 509, doi:10.1029/2006EO460001.

Fukasawa, M., H. Freeland, R. Perkin, T. Watanabe, H. Uchida, and A. Nishina (2004), Bottom water warming in the North Pacific Ocean, *Nature*, *427*(6977), 825–827, doi:10.1038/nature02337.

Gosselin, M., M. Levasseur, P. A. Wheeler, R. A. Horner, and B. C. Booth (1997), New measurements of phytoplankton and ice algal production in the Arctic Ocean, *Deep Sea Res. Part II*, *44*(8), 1623–1644, doi:10.1016/S0967-0645(97)00054-4.

Gregg, W. W., and K. L. Carder (1990), A simple spectral solar irradiance model for cloudless maritime atmospheres, *Limnol. Oceanogr.*, *35*(8), 1657–1675.

Harrison, W., and G. Cota (1991), Primary production in polar waters: Relation to nutrient availability, *Polar Res.*, *10*(1), 87–104, doi:10.1111/j.1751-8369.1991.tb00637.x.

Hill, V., and G. Cota (2005), Spatial patterns of primary production on the shelf, slope and basin of the western Arctic in 2002, *Deep Sea Res. Part II*, *52*(24–26), 3344–3354, doi:10.1016/j.dsr2.2005.10.001.

Holloway, G., and T. Sou (2002), Has Arctic sea ice rapidly thinned?, *J. Clim.*, *15*(13), 1691–1701, doi:10.1175/1520-0442(2002)015<1691:HASIRT>2.0.CO;2.

Intergovernmental Panel on Climate Change (2007), *Climate Change 2007—The Physical Science Basis: Working Group I Contribution to the Fourth Assessment Report of the IPCC Intergovernmental Panel on Climate Change*, Cambridge Univ. Press, New York.

Jakobsson, M., A. Grantz, Y. Kristoffersen, and R. Macnab (2003), Physiographic provinces of the Arctic Ocean seafloor, *Geol. Soc. Am. Bull.*, *115*(12), 1443–1455, doi:10.1130/B25216.1.

Jakobsson, M., R. Macnab, M. Mayer, R. Anderson, M. Edwards, J. Hatzky, H.-W. Schenke, and P. Johnson (2008), An improved bathymetric portrayal of the Arctic Ocean: Implications for ocean modeling and geological, geophysical and oceanographic analyses, *Geophys. Res. Lett.*, *35*, L07602, doi:10.1029/2008GL033520.

Johannessen, O., E. Shalina, and M. Miles (1999), Satellite evidence for an Arctic sea ice cover in transformation, *Science*, *286*(5446), 1937–1939, doi:10.1126/science.286.5446.1937.

Kirk, J. T. O. (1983), *Light and Photosynthesis in the Aquatic Ecosystems*, Cambridge Univ. Press, Cambridge, U. K.

Laxon, S., N. Peacock, and D. Smith (2003), High interannual variability of sea ice thickness in the Arctic region, *Nature*, *425*(6961), 947–950, doi:10.1038/nature02050.

Legendre, L., S. F. Ackley, G. S. Dieckmann, B. Gullicksen, R. Horner, T. Hoshiai, I. A. Melnikov, W. S. Reeburgh, M. Spindler, and C. W. Sullivan (1992), Ecology of sea ice biota: Part 2. Global significance, *Polar Biol.*, *12*, 429–444.

Levi, B. G. (2000), The decreasing Arctic ice cover, *Phys. Today*, *53*(1), 19–20, doi:10.1063/1.882931.

Macdonald, R. (1996), Awakenings in the Arctic, *Nature*, *380*(6572), 286–287, doi:10.1038/380286a0.

Macdonald, R. W., S. M. Solomon, R. E. Cranston, H. E. Welch, M. B. Yunker, and C. Gobeil (1998), A sediment and organic carbon budget for the Canadian Beaufort shelf, *Mar. Geol.*, *144*(4), 255–273, doi:10.1016/S0025-3227(97)00106-0.

Markus, T., and B. A. Burns (1995), A method to estimate subpixel-scale coastal polynyas with satellite passive microwave data, *J. Geophys. Res.*, *100*, 4473–4487, doi:10.1029/94JC02278.

Maslowski, W., D. Marble, W. Walczowski, U. Schauer, J. L. Clement, and A. J. Semtner (2004), On climatological mass, heat, and salt transports through the Barents Sea and Fram Strait from a pan-Arctic coupled ice-ocean model simulation, *J. Geophys. Res.*, *109*(C3), C03032, doi:10.1029/2001JC001039.

Matrai, P., M. Vernet, and P. Wassmann (2007), Relating temporal and spatial patterns of DMSP in the Barents Sea to phytoplankton biomass and productivity, *J. Mar. Syst.*, *67*, 83–101, doi:10.1016/j.jmarsys.2006.10.001.

Matsuoka, A., S. Saitoh, and K. Shimada (2005), A new approach for ocean color algorithm in Case 2 water using bio-optical field measurements in the western Arctic Ocean, *Proc. SPIE Int. Soc. Opt. Eng.*, *5977*, 77–87.

McLaughlin, F., K. Shimada, E. Carmack, M. Itoh, and S. Nishino (2005), The hydrography of the southern Canada Basin, 2002, *Polar Biol.*, *28*(3), 182–189, doi:10.1007/s00300-004-0701-6.

Menard, H. W., and S. M. Smith (1966), Hypsometry of ocean basin provinces, *J. Geophys. Res.*, *71*(18), 4305–4325.

Morales-Maqueda, M. A., A. J. Willmott, and M. S. Darby (1999), A numerical model for interdecadal variability of sea ice cover in the Greenland-Iceland-Norwegian Sea, *Clim. Dyn.*, *15*(2), 89–113, doi:10.1007/s003820050270.

Morel, A. (1978), Available, usable, and stored radiant energy in relation to marine photosynthesis, *Deep Sea Res.*, *25*(8), 673–688, doi:10.1016/0146-6291(78)90623-9.

Morel, A. (1987), Chlorophyll-specific scattering coefficient of phytoplankton a simplified theoretical approach, *Deep Sea Res. Part A*, *34*(7), 1093–1106, doi:10.1016/0198-0149(87)90066-5.

Morel, A. (1991), Light and marine photosynthesis: A spectral model with geochemical and climatological implications, *Prog. Oceanogr.*, *26*(3), 263–306, doi:10.1016/0079-6611(91)90004-6.

Niebauer, H., V. Alexander, and S. Henrichs (1990), Physical and biological oceanographic interaction in the spring bloom at the Bering Sea marginal ice edge zone, *J. Geophys. Res.*, *95*(C12), 22,229–22,241, doi:10.1029/JC095iC12p22229.

O'Reilly, J., S. Maritorena, B. Mitchell, D. Siegel, K. Carder, S. Garver, M. Kahru, and C. McClain (1998), Ocean color chlorophyll algorithms for SeaWiFS, *J. Geophys. Res.*, *103*(C11), 24,937–24,953, doi:10.1029/98JC02160.

Parkinson, C. L. (2000), Variability of Arctic sea ice: The view from space, and 18-year record, *Arctic*, *53*, 341–358.

Peterson, B. J., R. M. Holmes, J. W. McClelland, C. J. Vorosmarty, R. B. Lammers, A. I. Shiklomanov, I. A. Shiklomanov, and S. Rahmstorf (2002), Increasing river discharge to the Arctic Ocean, *Science*, *298*(5601), 2171–2173, doi:10.1126/science.1077445.

Peterson, B. J., J. McClelland, R. Curry, R. M. Holmes, J. E. Walsh, and K. Aagaard (2006), Trajectory shifts in the Arctic and subarctic freshwater cycle, *Science*, *313*(5790), 1061–1066, doi:10.1126/science.1122593.

Platt, T., W. G. Harrison, B. Irwin, E. P. Horne, and C. L. Gallegos (1982), Photosynthesis and photoadaptation of marine phytoplankton in the Arctic, *Deep Sea Res.*, *29*(10), 1159–1170, doi:10.1016/0198-0149(82)90087-5.

Reynolds, R. W., N. A. Rayner, T. M. Smith, D. C. Stokes, and W. Wang (2002), An improved in situ and satellite SST analysis for climate, *J. Clim.*, *15*, 1609–1625, doi:10.1175/1520-0442(2002)015<1609:AIISAS>2.0.CO;2.

Richter-Menge, J., et al. (2006), State of the Arctic Report, NOAA OAR special report, 36 pp., NOAA/OAR/PMEL, Seattle, Wash.

Rigor, I. G., and J. M. Wallace (2004), Variations in the age of Arctic sea ice and summer sea ice extent, *Geophys. Res. Lett.*, *31*(9), L09401, doi:10.1029/2004GL019492.

Rigor, I. G., J. M. Wallace, and R. L. Colony (2002), Response of sea ice to the Arctic Oscillation, *J. Clim.*, *15*(18), 2648, doi:10.1175/1520-0442(2002)015<2648:ROSITT>2.0.CO;2.

Rothrock, D. A., Y. Yu, and G. A. Maykut (1999), Thinning of the Arctic sea ice cover, *Geophys. Res. Lett.*, *26*(23), 3469, doi:10.1029/1999GL010863.

Rothrock, D. A., J. Zhang, and Y. Yu (2003), The arctic ice thickness anomaly of the 1990s: A consistent view from observations and models, *J. Geophys. Res.*, *108*(C3), 3083, doi:10.1029/2001JC001208.

Sakshaug, E. (2003), Primary and secondary production in the Arctic Seas, in *The Organic Carbon Cycle in the Arctic Ocean*, edited by R. Stein and R. W. Macdonald, pp. 57–81, Springer-Verlag, Berlin.

Sakshaug, E., K. Andresen, S. Myklestad, and Y. Olsen (1983), Nutrient status of phytoplankton communities in Norwegian waters (marine, brackish and fresh) as revealed by their chemical composition, *J. Plankton Res.*, *5*(2), 175–196, doi:10.1093/plankt/5.2.175.

Semiletov, I. P., A. Makshtas, S.-I. Akasofu, and E. Andreas (2004), Atmospheric CO_2 balance: The role of Arctic sea ice, *Geophys. Res. Lett.*, *31*, L05121, doi:10.1029/2003GL017996.

Serreze, M. C., J. A. Maslanik, T. A. Scambos, F. Fetterer, J. Stroeve, K. Knowles, C. Fowler, S. Drobot, R. G. Barry, and T. M. Haran (2003), A record minimum arctic sea ice extent and area in 2002, *Geophys. Res. Lett.*, *30*(3), 1110, doi:10.1029/2002GL016406.

Serreze, M. C., M. M. Holland, and J. Stroeve (2007), Perspectives on the Arctic's shrinking sea-ice cover, *Science*, *315*(5818), 1533–1536, doi:10.1126/science.1139426.

Shiklomanov, I. A. (2000), Appraisal and assessment of world water resources, *Water Int.*, *25*(1), 11–32.

Shimada, K., T. Kamoshida, M. Itoh, S. Nishino, E. Carmack, F. McLaughlin, S. Zimmermann, and A. Proshutinsky (2006), Pacific Ocean inflow: Influence on catastrophic reduction of sea ice cover in the Arctic Ocean, *Geophys. Res. Lett.*, *33*(8), L08605, doi:10.1029/2005GL025624.

Smith, D. M. (1998), Recent increase in the length of the melt season of perennial Arctic sea ice, *Geophys. Res. Lett.*, *25*(5), 655–658, doi:10.1029/98GL00251.

Steele, M., and W. Ermold (2004), Salinity trends on the Siberian shelves, *Geophys. Res. Lett.*, *31*(24), L24308, doi:10.1029/2004GL021302.

Subba Rao, D. V., and T. Platt (1984), Primary productivity of Arctic waters, *Polar Biol.*, *3*, 191–201, doi:10.1007/BF00292623.

Thompson, D. W. J., and J. M. Wallace (1998), Arctic Oscillation signature in the wintertime geopotential height and temperature fields, *Geophys. Res. Lett.*, *25*(9), 1297–1300, doi:10.1029/98GL00950.

Tremblay, J.-E., Y. Gratton, J. Fauchot, and N. M. Price (2002), Climatic and oceanic forcing of new, net, and diatom production in the North Water, *Deep Sea Res. Part II*, *49*(22–23), 4927–4946, doi:10.1016/S0967-0645(02)00171-6.

Ukita, J., M. Honda, H. Nakamura, Y. Tachibana, D. J. Cavalieri, C. L. Parkinson, H. Koide, and K. Yamamoto (2007), Northern Hemisphere sea ice variability: Lag structure and its implications, *Tellus Ser. A*, *59*(2), 261–272, doi:10.1111/j.1600-0870.2006.00223.x.

Vedernikov, V. I., A. B. Demidov, and A. I. Sudbin (1994), Primary production and chlorophyll in the Kara Sea in September 1993, *Oceanology Engl. Transl.*, *34*(5), 693–703.

Walsh, J. J., et al. (2005), A numerical model of seasonal primary production within the Chukchi/Beaufort seas, *Deep Sea Res. Part II*, *52*(24–26), 3541–3576, doi:10.1016/j.dsr2.2005.09.009.

Wang, J., and G. F. Cota (2003), Remote-sensing reflectance in the Beaufort and Chukchi seas: Observations and models, *Appl. Opt.*, *42*(15), 2754, doi:10.1364/AO.42.002754.

Wanner, H., S. Bronnimann, C. Casty, D. Gyalistras, J. Luterbacher, C. Schmutz, D. B. Stephenson, and E. Xoplaki (2001), North Atlantic Oscillation—Concepts and studies, *Surv. Geophys.*, *22*(4), 321–382, doi:10.1023/A:1014217317898.

Wassmann, P., and D. Slagstad (1993), Seasonal and annual dynamics of particulate carbon flux in the Barents Sea: A model approach, *Polar Biol.*, *13*(6), 363–372, doi:10.1007/BF01681977.

Zhang, J. L., D. Rothrock, and M. Steele (2000), Recent changes in Arctic sea ice: The interplay between ice dynamics and thermodynamics, *J. Clim.*, *13*(17), 3099–3114, doi:10.1175/1520-0442(2000)013<3099:RCIASI>2.0.CO;2.

Zuidema, P., E. R. Westwater, C. Fairall, and D. Hazen (2005), Ship-based liquid water path estimates in marine stratocumulus, *J. Geophys. Res.*, *110*, D20206, doi:10.1029/2005JD005833.

K. R. Arrigo, S. Pabi, and G. L. van Dijken, Department of Environmental Earth System Science, Stanford University, Stanford, CA 94305, USA. (arrigo@stanford.edu)